Low Temperature Physics/Fizika Nizkikh Temperatur, 2021, vol. 47, No. 7, pp. 577–595

Superlattice on the surface of a nanotube

(Review Article)

A. M. Ermolaev and G. I. Rashba

Academician I. M. Lifshitz Theoretical Physics Department

V. N. Karazin Kharkiv National University, Kharkiv 61022, Ukraine
E-mail: georgiy.i.rashba@gmail.com

Received February 13, 2021, published online May 26, 2021

The results of theoretical studies of the thermodynamic, kinetic, and high-frequency properties of the electron gas on the surface of a nanotube in a magnetic field in the presence of a longitudinal superlattice are presented. Nanodimensions of the motion area lead to energy quantization. Its multiply connected structure in the presence of a magnetic field leads to effects that are derived from the Aharonov–Bohm effect. It is shown that the curvature of a nanotube, even in the absence of a magnetic field, causes new macroscopic oscillation effects such as de Haas–van Alphen oscillations, which are associated with the quantization of the transverse electron motion energy and with the root peculiarities of the density of electron states on the nanotube surface. Thermodynamic potentials and heat capacity of the electron gas on the tube are calculated in the gas approximation. The Kubo formula for the conductivity tensor of the electron gas on the nanotube surface is obtained. The Landau damping regions of electromagnetic waves on a tube are determined and the beats are theoretically predicted on the graph of the dependence of conductivity on tube parameters. In the hydrodynamic approximation, the plasma waves on the surface of a semiconductor nanotube with a superlattice are considered. It is shown that optical and acoustic plasmons can propagate along a tube with one kind of carrier. Electron spin waves on the surface of a semiconductor nanotube with a superlattice in a magnetic field are studied. The spectra and areas of collisionless damping of these waves are found. We have shown that the spin wave damping is absent in these areas if the tubes with a degenerate electron gas have small radius.

Keywords: nanotubes, superlattice, magnetic field, thermodynamic functions, dynamic conductivity, plasma waves, electron spin waves.

Contents

1. Introduction

In the sixties of the last century, Moisey Isaakovich Kaganov, working on the book [1], could not ignore the promising direction in solid state physics – semiconductors with superlattices, which was rapidly developing. Superlattice is an additional translational symmetry artificially created on the surface and in the sample volume.

The physical properties of materials with an additional artificially created periodic structure (superlattice) differ significantly from the corresponding properties of homogeneous bodies. The additional potential of the superlattice modifies the band structure of the base material. Since the period of the quantum superlattice d is much larger than the lattice constant, the Brillouin zone is divided into a number of minibands. This creates narrow subbands (minibands) separated by forbidden regions in the conduction band and the valence band of the initial crystal. However, for such periodicity to significantly affect the behavior of quasiparticles (electrons, phonons, magnons), certain conditions must be met. First, the average energy of a quasiparticle should be comparable with the miniband width, and second, the superlattice period should be much less than the quasiparticle mean free path l: $d \ll l$. This inequality can be rewritten as $\Delta \gg \hbar/\tau$, where Δ is the half-width of the miniband, τ is the relaxation time. Superlattices, in which the above conditions are satisfied, are called quantum superlattices.

The idea of creating a quantum superlattice was first expressed by L. V. Keldysh [2], who proposed to use a powerful ultrasonic wave to obtain additional periodic potential. The first samples of quantum superlattices were synthesized as early as 1971 by the molecular epitaxy method [3, 4]. Continuous progress of methods of molecular beam epitaxy from metallic-organic compounds made it possible to create high-quality heterostructures based on the GaAs-$Ga_{1-x}Al_xAs$ system [5]. Currently superlattices are the main elements of a new technology called band-gap engineering.

The main results obtained by Moisey Isaakovich in this area are published in Refs. 6–10. In Ref. 6 the theory of acoustoelectronic interaction in crystals with superlattices is developed. Reference 7 contains the calculation of the thermodynamic quantities of superlattices in a magnetic field: chemical potential, magnetic moment, and sample temperature for a nondegenerate and degenerate electron gas. Oscillations in temperature are also found in this article. They are used as a method for adiabatic cooling of the sample. Reference 8 is devoted to the theory of electrical conductivity of semiconductors with superlattices in a quantizing magnetic field. This paper shows that a change in the quantizing magnetic field applied along the axis of a one-dimensional superlattice induces metal-dielectric phase transitions. Also in this paper, the characteristics of the photoconductivity of the superlattice in a quantizing magnetic field are calculated. In Ref. 9, the spectrum of low-frequency electromagnetic oscillations in a superlattice was calculated under the conditions of the quantum Hall effect and an assumption was made about the possibility of experimental detection of these waves in Hall dielectrics. A popular presentation of the basic ideas of the physics of semiconductors with superlattices is contained in the book [10].

The properties of massive semiconductors with superlattices are considered in many publications by domestic and foreign authors. Extensive reviews and monographs have been written, they describe a number of important aspects of superlattice physics [11–17].

The advances in modern nanoelectronics are associated both with the development of technology and with advances in fundamental physics, describing the thermodynamic and high-frequency properties of nanostructures. Advances in physics and the technology of solid-state nanostructures have led to the creation of a scientific foundation for their widespread use in nanoelectronics [18]. In this regard, the techniques and methods well known in the theory of massive semiconductors with superlattices, being applied to nanoobjects, are filled with new content. Solid-state nanostructures are nano-sized objects characterized by the presence of inhomogeneities of various nature and configurations within semiconductor and dielectric media. The range of these nanostructures is quite wide: quantum wires [18, 19], quantum dots [18, 20], fullerenes and nanotubes [21]. Although these objects differ in their physical nature, they are united by their very small size in one or several directions. These dimensions are only one or two orders of magnitude larger than the characteristic interatomic distance. Under these conditions, the quantum nature of the motion of current carriers manifests itself in an essential way. It is well known that the reception, transmission and processing of information in monomolecular structures are based on quantum processes of charge transfer in them. This circumstance leads to the widespread usage in scientific literature of such terms, as quantum computers, quantum information systems. The physical mechanisms, used in these structures, are the tunneling effect and the interaction of charged quasiparticles (conduction electrons) with a periodic potential, they have also been encountered earlier in solid state physics and the theory of massive superlattices. However, as applied to nanotubes, the nature of these effects significantly changes due to the quasi-one-dimensional type of conductivity and tube curvature. Therefore, the known results, related to 3D macroscopic samples, cannot be transferred to nanotubes. Thus, there is a need for new fundamental studies of thermodynamic and electromagnetic processes in quasi-1D macromolecules in general and in nanotubes in particular.

The purpose of this review article is to summarize the results of the authors' investigations in the field of the physical properties of nanotubes with superlattices. These studies cover the thermodynamics of nanotubes [22], dynamic conductivity [23, 24], collective excitations

(plasmons and Landau–Silin spin waves) of the electron gas of nanotubes with a longitudinal superlattice [25–34] and are based on a unified approach. The approach developed here uses the analogy between physical processes in nanotubes with superlattices and processes in massive superlattices, which were studied by M. I. Kaganov [6–10]. The review material is presented using a number of important problems in the physics of nanotubes as examples. It should be emphasized that the problems considered as a complex, in addition to theoretical and applied interest, serve as bright illustration of the general trends in the development of modern physics of nanostructures.

2. Nanotubes with superlattices: classification and research development

2.1. Classification of nanotubes

Thirty years have passed since the discovery of carbon nanotubes by Iijima [35]. However, the interest in these nanosystems is so great that in recent years a new direction in physics and technology has emerged – carbon nanomaterial science. Nanotubes are prepared by rolling up a graphene sheet (or two-dimensional heterostructure) into a tube. Depending on the rolling-up manner, the tube has metallic, semiconductor, or dielectric properties. Many articles and reviews have appeared in the world of scientific literature (see, for example, [36–38]), in which the properties of nanotubes are studied. They are interesting to physicists because nanotubes are dielectric, semiconductor, metal, so the methods developed to study these systems are transferred to nanotubes and other electron nanosystems on curved surfaces [38]. To study their properties, it is necessary to synthesize the methods of quantum mechanics, statistics and kinetics and Riemannian geometry. A new parameter appearing in theory (the curvature of the structure) contributes to enriching the picture of phenomena in nanosystems increasing the ways to control their properties. In electronic systems on curved surfaces, effects have already been discovered that have no analogue in systems with flat geometry. These include effects of hybridization of size and magnetic quantization of the motion of conduction electrons, modification of the electron Hamiltonian [38], specific resonances in the scattering of electrons in carbon nanotubes [39] and quantum wires [19] by impurity atoms.

The logic behind the development of solid state physics is such that currently the objects of investigations are not only three dimensional systems with superlattices [6–17], but also low-dimensional systems. Modern technologies allow creating not only nanotubes but nanotubes with superlattices. Along with flat superlattices [2, 4, 40–45], also ones with cylindrical symmetry exist [18]. They are of radial and longitudinal types [18, 46]. The radial superlattice is a set of coaxial cylinders, while the longitudinal one looks like a set of coaxial rings of the same radius. The tubes with longitudinal superlattice are prepared by lithographic methods. It can be obtained by embedding fullerenes or other additives to the nanotube or when the nanotube is attached to a substrate for charge exchange [47]. In such a system, there exists the periodic potential acting upon electrons moving along the tube.

2.2. Thermodynamics of nanotubes

The thermodynamic functions of electron gas on a nanotube surface have been studied in literature [48–54]. In Ref. 51 the geometrical effects in ideal quantum gases of electrons, photons and phonons in confined space were considered. In Ref. 52 a thermodynamic analysis of the boron-nitride nanotubes nucleation on the catalysts surface was performed. In Refs. 53, 54 the chemical potential, energy, pressure and the work function of an electronic gas on a conducting carbon nanotube surface under zero temperature are calculated. Within the framework of the Hartree–Fock approximation the contact electron-electron interaction is taken into account. Analytical form of the work function of carbon nanotubes was derived in the paper [54]. At large radii of nanotubes the limit to the work function of graphene was done.

Superlattice at the surface of a carbon nanotube has been previously studied [55, 56]. In Ref. 56 authors estimated orbital magnetization of the electron gas at the surface of the nanotube with the superlattice in a magnetic field parallel to the axes of the tube and the superlattice. Using the model suggested by the authors [56], we calculated the heat capacity of the degenerate electron gas [22]. In Subsections 4.1, 4.2 we present the results of calculations of such thermodynamic functions of the degenerate and nondegenerate electron gas on the semiconductor cylindrical nanotube surface in a longitudinal magnetic field as chemical potential, internal energy and heat capacity. We employ the effective mass approximation and Poisson summation formula for the calculation of the density of states [22].

2.3. Response function

Simplified conductivity models are usually used for studying electromagnetic waves propagation in the cylindrical geometry systems, for example, in nanotubes. The metal cylinder conductivity is often believed to be endless, and the dielectric permittivity of the matter in which cylinder is dipped is considered to be constant or only frequency dependent. Conductivity's spatial dispersion is usually not taken into account. Nonetheless, the electromagnetic field's nature in the tube, its waveguide characteristics are sensitive to the surface currents. Therefore, the electron gas conductivity tensor components calculation problem with allowance for the spatial and time dispersion is worth consideration. In connection with increased interest in currents within the cylindrical conductors, the authors of Ref. 57 have calculated the longitudinal conductivity for solid and hollow cylinders without superlattice in magnetic

field and considered quantum electromagnetic waves in such systems. Exact expressions for all the components of the conductivity tensor for degenerate and nondegenerate electron gas on the nanotube surface without superlattice are presented in Ref. 58. It is worth to be clarified how the superlattice affects this tensor. In Section 5.1, the components of the dynamic conductivity tensor are calculated based on the effective mass model for a nanotube with a longitudinal superlattice in a magnetic field. The superlattice axis and the magnetic field strength vector are assumed to be parallel to the tube axis.

The reaction of the electron gas of a nanotube to a weak alternating magnetic field is characterized by the tensor of dynamic magnetic susceptibility. The components of the magnetic susceptibility tensor presented in Subsection 5.2 will be used to solve the dispersion equation to determine the spectrum of Landau–Silin spin waves on a tube with a superlattice in Subsection 6.2 [27].

2.4. Collective excitations

Plasma waves on the surface of carbon [35] and semiconductor nanotubes [59, 60] were studied in [61–67]. Plasmon in the nanotubes are studied mainly in approximation of random phases [34, 62, 66, 67] and in the hydrodynamic approximation [65, 68]. In the framework of the hydrodynamic approach, the plasma waves on the surface of a nanotube with a longitudinal superlattice in Subsection 6.1 are considered. Not only longitudinal, but also transverse electron currents are taken into account. It was shown that both optical and acoustic plasmons can propagate through a tube with one type of carriers [32].

Electron spin waves on the surface of a semiconductor nanotube with a superlattice in a magnetic field have been considered in the Subsection 6.2. These waves in bulk conductors were predicted by Landau [69] and Silin [70]. Their properties in bulk conductors were considered in Refs. 71–73. Subsection 6.2 discusses spin-wave spectra on the surface of a nanotube with a superlattice and regions of collisionless damping of waves. It is shown that spin waves are not damped in small-radius tubes with a degenerate electron gas [31].

3. Electron energy spectrum and density of states on the nanotube surface with superlattice

3.1. Electron energy spectrum

The conduction electron energy spectrum in the carbon and semiconductor nanotubes has a band nature. A small electron density near the band edge permits to use the effective mass approximation. This approximation allows describing the properties of such systems qualitatively and often also quantitatively.

Energy of electron with effective mass m_* on the surface of a cylindrical nanotube with radius a with longitudinal superlattice consists of the energy of rotational motion, $l^2/2m_*a^2$, and that of longitudinal motion $\Delta(1-\cos kd)$, where $l=0,\pm1,...$ and k are projections of electron angular moment and momentum, respectively, onto the axis of the tube. The expression $\Delta(1-\cos kd)$ is usually used in the tight-binding model of electrons in a crystal lattice [1, 7, 8, 10, 11, 13–15]. Here Δ and d are, respectively, amplitude and period of modulating potential on the tube surface. If $kd \ll 1$, this expression becomes $k^2/2m$, where $m_* = 1/\Delta d^2$. Hereinafter, the Planck's constant is set to unity. In the magnetic field B, parallel to the tube axis Z, the energy of electron rotational motion becomes equal to $\varepsilon_0(l+\eta)^2$ [74], where $\varepsilon_0 = (2m_*a^2)^{-1}$ is the rotational quantum, $\eta = \Phi/\Phi_0$ is the ratio of magnetic flux $\Phi = \pi a^2 B$ through the tube cross-section to the flux quantum, $\Phi_0 = 2\pi c/e$ (e is the electron charge, c is the velocity of light). Taking into consideration the spin splitting of levels, we obtain the electron energy

$$\varepsilon_{lk\sigma} = \varepsilon_0\left(l+\eta\right)^2 + \Delta\left(1-\cos kd\right) + \sigma\mu_B B, \qquad (3.1)$$

where μ_B is the magnetic moment of an electron, $\sigma = \pm 1$ corresponds to two spin orientations. The longitudinal effective mass of an electron is supposed to be equal to its transversal one. Flux ratio $\eta = \Phi/\Phi_0$ is included in Eq. (3.1) in the form of $l+\eta$. This allows limiting η to $0 \le \eta \le 1$. The order of miniband location depends on η. If $\eta < 1/2$, we have $\varepsilon_0\eta^2 < \varepsilon_{-1} < \varepsilon_{+1} < \varepsilon_{-2} < ...$ If $\eta > 1/2$ then $\varepsilon_{-1} < \varepsilon_0\eta^2 < \varepsilon_{-2} < ...$ Here the spin level splitting will not be taken into consideration. At $\eta < 1/2$ lower miniband is within $[\varepsilon_0\eta^2, \varepsilon_0\eta^2 + 2\Delta]$, and the next is within $[\varepsilon_{-1}, \varepsilon_{-1} + 2\Delta]$. Energy gap between them is equal to $\varepsilon_0(1-2\eta) - 2\Delta$. Width of the kth gap between $(k+1)$th and kth minibands $(k = 1, 3, ...)$ is equal to $\varepsilon_0 k(1-2\eta) - 2\Delta$. Usually in experiments with nanotubes of radius $a \sim 10^{-7}$–10^{-6} cm $\varepsilon_0 \gg \Delta$, and the relationship between fluxes in different fields is far less than unity, therefore minibands don't overlap. However, with an increase in tube radius their overlap is inevitable.

The effect of Coulomb interaction of electrons on the tube onto the energy spectrum to Hartree–Fock approximation was discussed in Ref. 75. Screening the electron-electron interactions was studied in Refs. 76, 77. The Hartree–Fock correction to the spectrum (3.1) in the model of contact interaction of electrons has a usual form $gn_{-\sigma}$ [78], where n_σ is the surface density of electrons with spin projection σ, g is the Fourier component of electron short-range interaction energy. In this case, the electron energy on the tube with a longitudinal superlattice is [27]

$$\varepsilon_{lk}^{\sigma} = \varepsilon_0\left(l+\eta\right)^2 + \Delta\left(1-\cos kd\right) + gn_{-\sigma} + \sigma\mu_B B. \quad (3.2)$$

The first term in Eq. (3.2) refers to the quantized levels of the circular motion of electrons on the tube in the magnet-

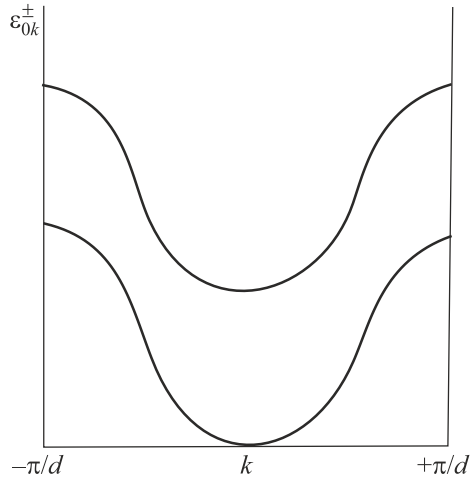

Fig. 1. Electron energy (3.1) in two overlapping minibands $0^{\pm}$.

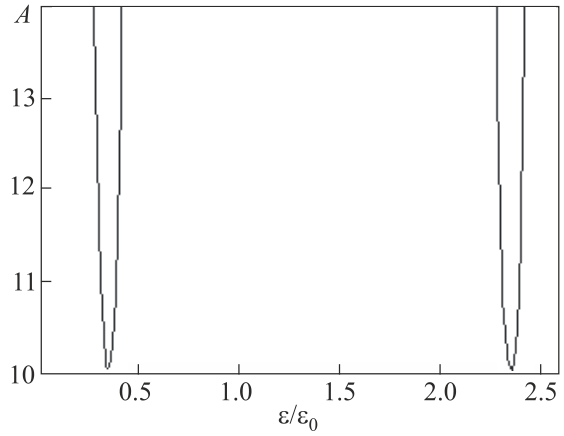

Fig. 2. Density of states (3.3) at the two lowest minibands of the spectrum (3.1) for parameter values given in the text.

ic field, the second term is the energy of the longitudinal motion of the electrons, and the third and fourth terms are the exchange shift and the spin splitting of the levels, respectively. The energy spectrum of the longitudinal motion of electrons consists of narrow minibands with the widths 2Δ separated by energy gaps. The minibands can overlap. Small-radius tubes correspond to the case with a small number of occupied lower minibands. Figure 1 shows schematically spectrum (3.1) in the first Brillouin zone ($-\pi/d < k < \pi/d$, when two lower spin-split minibands $0^{\pm}$ ($l = 0$, $\sigma = \pm 1$) overlap. We consider the case of $\eta < 1/2$ when the positions of the lower boundaries $\varepsilon^{\pm}_l$ of the minibands satisfy the inequalities $\varepsilon^{-}_0 < \varepsilon^{+}_0 < \varepsilon^{-}_{-1} < \varepsilon^{+}_{-1} < \ldots$ The miniband overlapping region $[\varepsilon^{+}_0, \varepsilon^{-}_0 + 2\Delta]$ in Fig. 1 has the width $2\Delta - \Omega$ with $\Omega = g\delta n + 2\mu B$, where $\delta n = n_{-} - n_{+}$.

3.2. Density of electron states

Electron density of states with the spectrum (3.1) is calculated according to the formula

$$\nu(\varepsilon) = \sum_{lk\sigma} \delta(\varepsilon - \varepsilon_{lk\sigma}).$$

This equals

$$\nu(\varepsilon) = \frac{L}{\pi d} \sum_{l\sigma} \frac{\Theta(\varepsilon - \varepsilon^{\sigma}_l)\theta(\varepsilon^{\sigma}_l + 2\Delta - \varepsilon)}{\sqrt{(\varepsilon - \varepsilon^{\sigma}_l)(\varepsilon^{\sigma}_l + 2\Delta - \varepsilon)}}. \qquad (3.3)$$

Here $\varepsilon^{\sigma}_l = \varepsilon^{\sigma}_{l0}$, L is the tube length, Θ is the Heaviside function. In the absence of a superlattice, Eq. (3.1) represents a system of one-dimensional subbands with root singularities of state density at their boundaries ε^{σ}_l. Modulating potential converts this spectrum to minibands 2Λ wide with boundaries ε^{σ}_l and $\varepsilon^{\sigma}_l + 2\Delta$. Figure 2 shows the dimensionless density of states $A = \pi \nu d \varepsilon_0 / 2L$ (3.3) in the two lower minibands of the spectrum (3.1) as a function of $\varepsilon/\varepsilon_0$ for parameters $\eta = 0.1$, $\Delta/\varepsilon_0 = 0.1$, usually used in experiments [56].

When $\varepsilon \gg \varepsilon_0$, the sum of l included in (3.3) can be substituted with an integral expression. As a result, the spectrum of the nanotubes becomes continuous, and density of states is now equal to

$$\nu(\varepsilon) = \begin{cases} \dfrac{4L}{\pi d\sqrt{2\Delta\varepsilon_0}} K\left(\sqrt{\dfrac{\varepsilon}{2\Delta}}\right), & \varepsilon < 2\Delta, \\ \dfrac{4L}{\pi d\sqrt{2\Delta\varepsilon\varepsilon_0}} K\left(\sqrt{\dfrac{2\Delta}{\varepsilon}}\right), & \varepsilon > 2\Delta, \end{cases} \qquad (3.4)$$

where $K(k)$ is the complete elliptic integral of the first kind with modulus k [79]. Considering the abovementioned relationship between m_* with Δ and d, we are reassured that (3.4) represents the density of states of a two-dimensional electron gas with a one-dimensional superlattice in the absence of a magnetic field, occupying a band with area $S = 2\pi aL$. This system can be obtained by cutting the tube along its length and turning it inside out to form a surface. If $\varepsilon \ll 2\Delta$ from (3.4) the density of states of a two-dimensional electron gas in the absence of a superlattice is obtained: $\nu_0 = m_* S/\pi$.

Poisson formula is used for the calculation of l, included in Eq. (3.3), at $\varepsilon \gg \varepsilon_0$. Then $\nu = \nu_{\text{mon}} + \nu_{\text{osc}}$, where ν_{mon} is the monotonic component of the density of states of Eq. (3.3), and ν_{osc} is the oscillating component. The latter contains Fourier integral with a finite limits, where integrand has a root singularity at the limits of integration. Asymptote of the far Fourier component of this integral is known [80]. From it we obtained

$$\nu_{\rm osc}(\varepsilon)=\frac{4L}{\pi d\varepsilon_0}\left(\frac{\varepsilon_0}{\varepsilon}\right)^{3/4}\left(\frac{\varepsilon}{2\Delta}\right)^{1/2}\sum_{l=1}^{\infty}\frac{1}{\sqrt{l}}\cos 2\pi l\frac{\Phi}{\Phi_0}\cos\left(2\pi l\sqrt{\frac{\varepsilon}{\varepsilon_0}}-\frac{\pi}{4}\right),\qquad \varepsilon_0\ll\varepsilon<2\Delta,$$

$$\nu_{\rm osc}(\varepsilon)=\frac{4L}{\pi d\varepsilon_0}\left(\frac{\varepsilon_0}{\varepsilon}\right)^{3/4}\left(\frac{\varepsilon}{2\Delta}\right)^{1/2}\sum_{l=1}^{\infty}\frac{1}{\sqrt{l}}\cos 2\pi l\frac{\Phi}{\Phi_0}\left[\cos\left(2\pi l\sqrt{\frac{\varepsilon}{\varepsilon_0}}-\frac{\pi}{4}\right)+\left(1-\frac{2\Delta}{\varepsilon}\right)^{-1/4}\cos\left(2\pi l\sqrt{\frac{\varepsilon}{\varepsilon_0}\left(1-\frac{2\Delta}{\varepsilon}\right)}+\frac{\pi}{4}\right)\right],\qquad (3.5)$$

$\varepsilon\gg\varepsilon_0,\quad \varepsilon>2\Delta.$

Function (3.5) oscillates with the change in electron energy and magnetic flux Φ. The amplitude of oscillations decreases with increase in energy proportionally to $\varepsilon^{-1/4}$.

4. Thermodynamic quantities of a nanotube with a superlattice

4.1. Degenerate electron gas

Using density of states (3.4) and (3.5) let us calculate the number of electrons N, their energy E, chemical potential μ and heat capacity C. Let us consider degenerate gas at the surface of the nanotube with a longitudinal superlattice.

In the case appropriate for nanotubes with a small radius, when at zero temperature electrons partially fill only the lower miniband, we obtained

$$N=\frac{4L}{\pi d}\arcsin\sqrt{\frac{\mu_0-\varepsilon_-}{2\Delta}},$$
$$E=\frac{4L}{\pi d}\Delta\left[\left(1+\frac{\varepsilon_-}{\Delta}\right)\arcsin\sqrt{\frac{\mu_0-\varepsilon_-}{2\Delta}}-\right.\qquad (4.1)$$
$$\left.-\frac{1}{2\Delta}\sqrt{(\mu_0-\varepsilon_-)(\varepsilon_-+2\Delta-\mu_0)}\right].$$

Here $\varepsilon_-=\varepsilon_0\eta^2$ is the lower limit of spectrum (3.1), μ_0 is the Fermi energy. From Eq. (4.1) Fermi energy is found

$$\mu_0=\varepsilon_-+2\Delta\sin^2\frac{\pi d n_{\rm lin}}{4}.$$

The energy of a completely filled miniband is equal

$$E=\frac{2L\Delta}{d}\left(1+\frac{\varepsilon_-}{\Delta}\right),$$

where $n_{\rm lin}=N/L$ is linear electron density.

In order to obtain heat capacity of electron gases one must perform Sommerfeld expansion [81, 82] of the functions N and E of powers of T/μ, where T is the temperature (Boltzmann constant equal unity is assumed). This is possible if the chemical potential is located far from the features of state densities, i.e., the following inequalities must be met

$$T\ll\mu-\varepsilon_-,\quad T\ll\varepsilon_+-\mu,\qquad (4.2)$$

where $\varepsilon_\pm$ are the upper and lower boundaries of the last partially filled miniband. Corrections on the order of T^2 in expansion of N and E are equal

$$N_T=\frac{\pi LT^2}{3d}(\mu_0-\varepsilon_-+\Delta)\left[(\mu_0-\varepsilon_-)(\varepsilon_+-\mu_0)\right]^{-3/2},$$
$$E_T=\frac{\pi LT^2}{3d}\left[\mu_0\Delta-\varepsilon_-(\varepsilon_+-\mu_0)\right]\left[(\mu_0-\varepsilon_-)(\varepsilon_+-\mu_0)\right]^{-3/2}.$$

If $T\ll\mu_0-\varepsilon_-\ll 2\Delta$ then corrections in chemical potential and energy due to temperature are equal

$$\delta\mu=\frac{\pi^2T^2}{12(\mu_0-\varepsilon_-)},$$
$$\delta E=\frac{\pi L\Delta T^2}{3d(2\Delta)^{3/2}\sqrt{\mu_0-\varepsilon_-}}.\qquad (4.3)$$

δE takes into account a term present due to the dependence of chemical potential on temperature. From (4.3) we obtained monotonic component of the nanotube's heat capacity

$$C_{\rm mon}=\frac{\pi LT}{3d\sqrt{2\Delta}\sqrt{\mu_0-\varepsilon_-}}.\qquad (4.4)$$

Using Eq. (3.4) heat capacity of an electron gas with a superlattice in the absence of a magnetic field at low temperatures can be obtained. If $\mu_0<2\Delta$ heat capacity equals

$$C=\frac{TS}{3d}\sqrt{\frac{m_*}{\Delta}}\left(1-\frac{\mu_0}{2\Delta}\right)^{-1}\left[E\left(\sqrt{\frac{\mu_0}{2\Delta}}\right)+\left(1-\frac{\mu_0}{2\Delta}\right)K\left(\sqrt{\frac{\mu_0}{2\Delta}}\right)\right],\qquad (4.5)$$

where $E(k)$ is the complete elliptic integral of the second kind [79]. Coefficient at T in this formula is calculated precisely. If $\mu_0\ll 2\Delta$, from Eq. (4.5) standard expression for the heat capacity of an electron gas without a superlattice is obtained: $C=\pi m_* TS/3$, where density of states ν_0 is used. In accord with the Pauli principle heat capacity (4.4) and (4.5) is proportional to the temperature. However, proportionality coefficient is a complex function of the μ_0/Δ parameter.

Oscillating components N and E at conditions (4.2) and $\varepsilon_0\ll\mu_0<2\Delta$ are equal

$$\begin{pmatrix}N_{\rm osc}\\E_{\rm osc}\end{pmatrix}=\frac{4(\varepsilon_0\mu_0)^{1/4}L}{\pi^2 d\sqrt{2\Delta}}\begin{pmatrix}1\\\mu_0\end{pmatrix}\times$$
$$\times\sum_{l=1}^{\infty}\frac{1}{l^{3/2}}\cos\left(2\pi l\frac{\Phi}{\Phi_0}\right)\sin\left(2\pi l\sqrt{\frac{\mu_0}{\varepsilon_0}}-\frac{\pi}{4}\right)\times\frac{\lambda_l}{\sinh\lambda_l},\qquad (4.6)$$

where $\lambda_l = \pi^2 lT/(\varepsilon_0\mu_0)^{1/2}$. Functions (4.6) experience oscillations similar to de Haas–van Alphen and Aharonov–Bohm type oscillations with changes in $\mu_0^{1/2}$ related to electron density and magnetic flux Φ. The first are due to passage of root singularity of state density (3.3) at miniband boundaries through Fermi energy. This brings oscillations in consideration closer to de Haas–van Alphen type oscillations in a magnetic field [81, 82]. However nonequidistance of energy levels of cross-sectional movement of electrons in the tube brings about $(\mu_0/\varepsilon_0)^{1/2}$ in phase with oscillations (4.6). These oscillations exist in absence of a magnetic field. Their period is equal to $\tau = 1/\sqrt{2m_*}a$. A measurement of the period allows one to obtain effective mass of an electron. Amplitude of oscillations decreases with an increase in temperature, as it does in the usual case of de Haas–van Alphen effect in a quantizing magnetic field [81, 82].

From Eq. (4.6) let us obtain the oscillating term of heat capacity of a nanotube:

$$C_{\text{osc}} = \frac{4\mu_0 L}{d\sqrt{2\Delta}(\varepsilon_0\mu_0)^{1/4}}\sum_{l=1}^{\infty}\frac{1}{\sqrt{l}}\cos\left(2\pi l\frac{\Phi}{\Phi_0}\right)\times$$

$$\times\sin\left(2\pi l\sqrt{\frac{\mu_0}{\varepsilon_0}}-\frac{\pi}{4}\right)\frac{1}{\sinh\lambda_l}(1-\lambda_l\coth\lambda_l). \qquad (4.7)$$

With an increase in temperature monotonic component of heat capacity (4.4) exceeds the oscillating component (4.7) if $T > \mu_0(\mu_0/\varepsilon_0)^{1/4}$.

Figure 3 illustrates dependence of the amplitude of the main harmonic of the oscillating component of heat capacity (4.7)

$$B = \frac{4}{\sqrt{2}}\frac{L}{d}\left(\frac{\varepsilon_0}{\Delta}\right)^{1/2}\left(\frac{\mu_0}{\varepsilon_0}\right)^{3/4}\frac{\lambda_l\coth\lambda_l - 1}{\sinh\lambda_l}$$

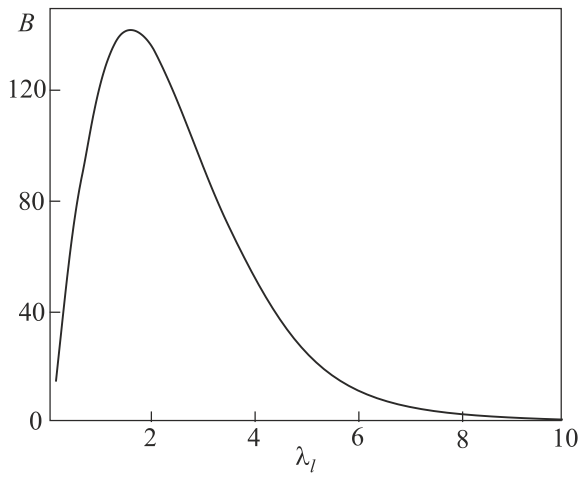

Fig. 3. Temperature dependence of the amplitude of the oscillating component of heat capacity (4.7) for parameter values given in the text.

on the temperature when $\Phi/\Phi_0 = 0.1$ for the values of GaAs parameters that are usually used in experiments [83]: $m_* = 0.07m_0$ (where m_0 is the mass of a free electron), $a = 10^{-6}$ cm, $\mu_0/\varepsilon_0 = 10$, $L = 10$ μm, $\Delta = 1$ meV, d = 3500 Å. Amplitude of B reaches its maximum value at temperature $T_m \propto (\varepsilon_0\mu_0)^{1/2}$ (α denotes proportionality).

4.2. Non-degenerate electron gas

At a fixed number of electrons chemical potential of a nondegenerate electron gas can be determined from equation

$$N = \sum_{mk\sigma}\exp\left[\beta(\mu - \varepsilon_{mk\sigma})\right], \qquad (4.8)$$

where β is the reverse temperature. Sums included in this expression are determined precisely. For estimating the sum by m the following formula is used [84]

$$\sum_{m=-\infty}^{\infty}\exp\left[-x(m+\upsilon)^2\right] = \sqrt{\frac{\pi}{x}}\sum_{l=-\infty}^{\infty}\exp\left(-\frac{\pi^2 l^2}{x}\right)\cos 2\pi l\upsilon,$$

$$x > 0$$

The sum by k is reduced to Bessel's modified function of the first kind [85]

$$I_0(x) = \frac{1}{\pi}\int_0^{\pi} d\phi\cdot e^{x\cdot\cos\phi}.$$

As a result, solution of Eq. (4.8) has the form

$$\mu = \frac{1}{\beta}\ln\left\{\frac{Nd}{2L}\sqrt{\frac{\beta\varepsilon_0}{\pi}}e^{\beta\Delta}\times\right.$$

$$\left.\times\left[\cosh\beta\mu_B B\cdot I_0(\beta\Delta)\left(1+2\sum_{l=1}^{\infty}\exp\left(-\frac{\pi^2 l^2}{\beta\varepsilon_0}\right)\cos 2\pi l\frac{\Phi}{\Phi_0}\right)\right]^{-1}\right\}. \qquad (4.9)$$

This shows that chemical potential undergoes Aharonov–Bohm type oscillations with a change in magnetic field crossing the tube. De Haas–van Alphen type oscillations are not present in this case. In the absence of a superlattice they were considered in article [86].

Energy of an electron gas can be calculated by equation [81, 82]

$$E = -N\frac{\partial}{\partial\beta}\ln\sum_{mk\sigma}\exp(-\beta\varepsilon_{mk\sigma}).$$

It equals

$$E = \frac{N}{2\beta}\left\{2\beta\varepsilon_0\left\langle\left(m+\frac{\Phi}{\Phi_0}\right)^2\right\rangle+\right.$$

$$\left.+1-2\beta\Delta\left[1-\frac{I_0'(\beta\Delta)}{I_0(\beta\Delta)}\right]-2\beta\mu_B B\,\text{th}\beta\mu_B B\right\}, \qquad (4.10)$$

where

$$\langle P_m \rangle = \frac{\sum_m P_m \exp(-\beta\varepsilon_m)}{\sum_m \exp(-\beta\varepsilon_m)}, \quad \varepsilon_m = \varepsilon_0 \left(m + \frac{\Phi}{\Phi_0} \right)^2 .$$

Derivative with respect to the argument of the Bessel function is marked with a prime (′).

Heat capacity of an electron gas equals

$$C = \frac{N}{2} \left\{ 2(\beta\varepsilon_0)^2 \left[\left\langle \left(m + \frac{\Phi}{\Phi_0} \right)^4 \right\rangle - \left\langle \left(m + \frac{\Phi}{\Phi_0} \right)^2 \right\rangle^2 \right] + \right.$$
$$+ 1 + 2(\beta\Delta)^2 \left[I_0''(\beta\Delta) I_0(\beta\Delta) - (I_0'(\beta\Delta))^2 \right] \times \qquad (4.11)$$
$$\left. \times \left[[I_0(\beta\Delta)]^{-2} + 2 \left(\frac{\beta\mu_B B}{\cosh \beta\mu_B B} \right)^2 \right] \right\}.$$

Separate terms in Eqs. (4.10) and (4.11) agree with the energy term in (3.1). The first term on the right side of expression (4.10) represents the average energy of centripetal motion of electrons at the surface of the nanotube, the second and third terms are due to longitudinal motion of electrons along the tube, and the last term is due to spin splitting of energy levels of an electron in a magnetic field. It coincides with the energy of a two-level system with distance $2\mu_B B$ between the levels. Expression (4.11) shows that the presence of a magnetic field does not affect the heat capacity term present due to electron motion. At the same time, modulation does not affect heat capacity related to centripetal motion of electrons and spin splitting of levels. Using the presentation of a Bessel function as a row and its asymptote, "longitudinal" component of heat capacity (4.11) is confirmed to be equal to

$$C_{\parallel} = \frac{N}{2} \left\{ 1 + 2(\beta\Delta)^2 \left[I_0''(\beta\Delta) I_0(\beta\Delta) - (I_0'(\beta\Delta))^2 \right] \times \right.$$
$$\left. \times [I_0(\beta\Delta)]^{-2} \right\} = \begin{cases} \frac{N}{2}, \beta\Delta \ll 1, \\ N, \beta\Delta \gg 1. \end{cases}$$

This result agrees with the classical theory on equipartition of energy about degrees of freedom [81]. Its physical meaning is obvious. If energy of thermal motion of electrons β^{-1} is small compared to the modulating potential amplitude, the electrons oscillate slightly in the modulating potential gaps. These oscillations make a contribution to heat capacity in the amount of N. If β^{-1} exceeds modulation amplitude Δ, the electrons move freely along the tube. Contribution of this motion to heat capacity is equal to $N/2$. Thus, term $C_{\parallel}$ changes from N to $N/2$ as temperature increases. "Transverse" part of heat capacity depends on the magnetic flux. In weak magnetic fields, the inequality holds $\Phi \ll \Phi_0$. This allows the dismissal of magnetic field influence on the "transverse" component of heat capacity $C_{\perp}$. Then the following limiting expressions can be obtained:

$$C_{\perp} = \begin{cases} N/2, & \beta\varepsilon_0 \ll 1, \\ N(\beta\varepsilon_0)^2 \exp(-\beta\varepsilon_0), & \beta\varepsilon_0 \gg 1. \end{cases}$$

As expected, high temperature limit of $C_{\perp}$ is in accord with the theorem on equipartition of energy about degrees of freedom.

5. Response function of electron gas on a tube with superlattice

5.1. Conductivity tensor

For the nanotube with superlattice in magnetic field, the surface electron gas linear response to an electromagnetic wave $\mathbf{E} = \mathbf{E}_0 \exp i(m\varphi + qz - \omega t)$ is characterized by conductivity two-dimensional tensor $\sigma_{\alpha\beta}(m, q, \omega)$. Here $\mathbf{E}$ is the electric field of wave, m is the integer number, q and ω are the wave vector and frequency of the wave, φ and z are cylindrical coordinates. The density of surface current on the tube is

$$j_\alpha(m, q, \omega) = \sum_\beta \sigma_{\alpha\beta}(m, q, \omega) E_\beta(m, q, \omega), \qquad (5.1)$$

where $j_\alpha(m, q, \omega)$ and $E_\beta(m, q, \omega)$ are cylindrical harmonics of $\mathbf{j}$ and $\mathbf{E}$ vectors. Kubo's formula for the conductivity tensor of electron gas on the surface of the nanotube with superlattice is [58]

$$\sigma_{\alpha\beta}(m, q, \omega) = \mathrm{i} \frac{e^2 n}{m_* \omega} \delta_{\alpha\beta} +$$
$$+ \frac{1}{\omega} \int_0^\infty dt\, \mathrm{e}^{\mathrm{i}\omega t} \left\langle \left[\hat{J}_\alpha(m, q, t), \hat{J}_\beta(-m, -q, 0) \right] \right\rangle , \qquad (5.2)$$

where n is surface density of electrons, $\mathbf{J}(m, q, t)$ is the cylindrical harmonics of current density operator in the external magnetic field $\mathbf{B}$. The angle brackets denote the average value of the operator commutator. The quantum constant was assumed as unity. The components of $\mathbf{J}(m, q)$ vector are

$$\hat{J}_\varphi = -\frac{2e}{m_* a \sqrt{S}} \sum_{lk} \left(l + \eta + \frac{m}{2} \right) \hat{a}_{lk}^+ \hat{a}_{(l+m)(k+q)},$$
$$\hat{J}_z = -\frac{2e}{m_* \sqrt{S}} \sum_{lk} \left(k + \frac{q}{2} \right) \hat{a}_{lk}^+ \hat{a}_{(l+m)(k+q)}, \qquad (5.3)$$

where $\hat{a}_{lk}$ and $\hat{a}_{lk}^+$ are operators of annihilation and creation of electrons in $|lk\rangle$ state, $S = 2\pi aL$ is the surface area for the tube with length L. Spin splitting of levels is not considered in Eq. (5.3).

From Eqs. (5.2) and (5.3) we obtain the components of conductivity tensor:

$$\sigma_{\varphi\varphi} = \mathrm{i}\frac{e^2 n}{m_*\omega} + \mathrm{i}\frac{2e^2}{m_*^2 a^2 \omega S}\sum_{lk} f\left(\varepsilon_{lk}\right)\times$$
$$\times\left[\frac{\left(l+\eta+\frac{m}{2}\right)^2}{\varepsilon_{lk}-\varepsilon_{(l+m)(k+q)}+\omega+\mathrm{i}0} - \frac{\left(l+\eta-\frac{m}{2}\right)^2}{\varepsilon_{(l-m)(k-q)}-\varepsilon_{lk}+\omega+\mathrm{i}0}\right], \quad (5.4)$$

$$\sigma_{\varphi z} = \sigma_{z\varphi} = \mathrm{i}\frac{2e^2}{m_*^2 a\omega S}\sum_{lk} f\left(\varepsilon_{lk}\right)\times$$
$$\times\left[\frac{\left(l+\eta+\frac{m}{2}\right)\left(k+\frac{q}{2}\right)}{\varepsilon_{lk}-\varepsilon_{(l+m)(k+q)}+\omega+\mathrm{i}0} - \frac{\left(l+\eta-\frac{m}{2}\right)\left(k-\frac{q}{2}\right)}{\varepsilon_{(l-m)(k-q)}-\varepsilon_{lk}+\omega+\mathrm{i}0}\right], \quad (5.5)$$

$$\sigma_{zz} = \mathrm{i}\frac{e^2 n}{m_*\omega} + \mathrm{i}\frac{2e^2}{m_*^2 \omega S}\sum_{lk} f\left(\varepsilon_{lk}\right)\times$$
$$\times\left[\frac{\left(k+\frac{q}{2}\right)^2}{\varepsilon_{lk}-\varepsilon_{(l+m)(k+q)}+\omega+\mathrm{i}0} - \frac{\left(k-\frac{q}{2}\right)^2}{\varepsilon_{(l-m)(k-q)}-\varepsilon_{lk}+\omega+\mathrm{i}0}\right]. \quad (5.6)$$

Here f is Fermi function,

$$\varepsilon_{lk} = \varepsilon_0\left(l+\eta\right)^2 + \Delta\left(1-\cos kd\right). \quad (5.7)$$

The second term addend in the right part of Eq. (5.7) is often used in the theory of semiconductor superlattices [7, 8, 10, 11–15]. The real parts of the components $\sigma_{\varphi\varphi}$ and σ_{zz} are even functions of m and ω, while imaginary parts are odd ones. At zero temperature in summation Σ_k the values k in the formulas (5.4)–(5.6) are limited to gap $-k_l \le k \le k_l$, where

$$k_l = \frac{1}{d}\arccos\frac{\varepsilon_l + \Delta - \mu_0}{\Delta}$$

is the maximum momentum of the electrons in the miniband l, $\varepsilon_l = \varepsilon_0(l+\eta)^2$ is the miniband boundaries. If $q = 0$, at zero temperature from the formulas (5.4)–(5.6) we calculate the components of dynamical conductivity tensor:

$$\mathrm{Re}\,\sigma_{\varphi\varphi}\left(m,\omega\right) = \frac{e^2}{\pi m_*^2 a^3\omega}\sum_l k_l\left[\left(l+\eta+\frac{m}{2}\right)^2\times\right.$$
$$\left.\times\delta\left(\omega-\Omega_+\right) - \left(l+\eta-\frac{m}{2}\right)^2\delta\left(\omega-\Omega_-\right)\right],$$
$$\mathrm{Im}\,\sigma_{\varphi\varphi}\left(m,\omega\right) = \frac{e^2 n}{m_*\omega} + \frac{e^2}{\pi^2 m_*^2 a^3\omega}\times \quad (5.8)$$
$$\times\sum_l k_l\left[\frac{\left(l+\eta+\frac{m}{2}\right)^2}{\omega-\Omega_+} - \frac{\left(l+\eta-\frac{m}{2}\right)^2}{\omega-\Omega_-}\right],$$
$$\sigma_{\varphi z}\left(m,\omega\right) = 0,$$

$$\mathrm{Re}\,\sigma_{zz}\left(m,\omega\right) = \frac{e^2}{3\pi m_*^2 a\omega}\sum_l k_l^3\left[\delta\left(\omega-\Omega_+\right)-\delta\left(\omega-\Omega_-\right)\right],$$
$$\mathrm{Im}\,\sigma_{zz}\left(m,\omega\right) = \frac{e^2 n}{m_*\omega} + \frac{e^2}{3\pi^2 m_*^2 a\omega}\sum_l k_l^3\left[\frac{1}{\omega-\Omega_+} - \frac{1}{\omega-\Omega_-}\right]. \quad (5.9)$$

Here $\Omega_\pm = \varepsilon_0 m[2(l+\eta)\pm m]$ are frequencies of direct transitions of electrons between the miniband boundaries ε_l in the field of electromagnetic wave. During the transitions, conservation laws for longitudinal components of angular moment, momentum, and energy are satisfied. At zero temperature, the summation over l in Eqs. (5.8) and (5.9) is limited by the condition $\left|\varepsilon_l + \Delta - \mu_0\right| \le \Delta$. This means that Fermi energy is concentrated within the miniband. The minibands are positioned in the intervals $[\varepsilon_l, \varepsilon_l + 2\Delta]$ and have the width 2Δ. Generally, the semiconductor nanotubes with radius $a \sim (10^{-7}$–$10^{-6})$ cm in magnetic field $B \sim 10^5$ G are used. In this case, the electrons of the semiconductor nanotube occupy little quantity of bottom minibands, which boundaries at $\eta < 1/2$ satisfy the inequality $\varepsilon_0\eta^2 < \varepsilon_{-1} < \varepsilon_1 < \varepsilon_{-2} < \ldots$ In the quantum limit where $n < 1/\pi ad$, Fermi energy is concentrated in the bottom miniband $l = 0$ $[\varepsilon_0\eta^2, \varepsilon_0\eta^2 + 2\Delta]$. In this case, in the absence of spatial dispersion, from Eqs. (5.8) and (5.9) we obtain

$$\mathrm{Re}\,\sigma_{\varphi\varphi} = \frac{e^2 k_0}{\pi m_*^2 a^3\omega}\times\left[\left(\eta+\frac{m}{2}\right)^2\delta\left(\omega-\varepsilon_0 m\left(2\eta+m\right)\right) - \left(\eta-\frac{m}{2}\right)^2\delta\left(\omega-\varepsilon_0 m\left(2\eta-m\right)\right)\left(\eta-\frac{m}{2}\right)^2\delta\left(\omega-\varepsilon_0 m\left(2\eta-m\right)\right)\right],$$
$$\mathrm{Im}\,\sigma_{\varphi\varphi} = \frac{e^2 n}{m_*\omega} + \frac{e^2 k_0}{\pi^2 m_*^2 a^3\omega}\left[\frac{\left(\eta+\frac{m}{2}\right)^2}{\omega-\varepsilon_0 m\left(2\eta+m\right)} - \frac{\left(\eta-\frac{m}{2}\right)^2}{\omega-\varepsilon_0 m\left(2\eta-m\right)}\right], \quad (5.10)$$

$$\mathrm{Re}\,\sigma_{zz} = \frac{e^2 k_0^3}{3\pi m_*^2 a\omega}\left[\delta\left(\omega-\varepsilon_0 m\left(2\eta+m\right)\right) - \delta\left(\omega-\varepsilon_0 m\left(2\eta-m\right)\right)\right],$$
$$\mathrm{Im}\,\sigma_{zz} = \frac{e^2 n}{m_*\omega} + \frac{e^2 k_0^3}{3\pi^2 m_*^2 a\omega}\left[\frac{1}{\omega-\varepsilon_0 m\left(2\eta+m\right)} - \frac{1}{\omega-\varepsilon_0 m\left(2\eta-m\right)}\right]. \quad (5.11)$$

Here $\Omega_{\pm} = \varepsilon_0 m(2\eta \pm m)$. The superlattice parameters Δ and d are included in Eqs. (5.10) and (5.11) only via the maximum momentum k_0 of electrons in the bottom miniband. In the absence of superlattice: $\Delta \to \infty$, $d \to 0$, $d^2\Delta \to m_*^{-1}$. Then $k_l = [2m_*(\mu - \varepsilon_l)]^{1/2}$ and the Eqs. (5.10) and (5.11) agree with ones obtained in Ref. 58. At $m = 0$, only the imaginary part $e^2 n/m_*\omega$ remains in Eqs. (5.10) and (5.11), while the real part is zero. This determines the electromagnetic wave energy absorbed by electrons. In the absence of direct and indirect transitions of electrons, the absorption is zero. As the electron density grows, the number of addends in Eqs. (5.8) and (5.9) increases. If Fermi energy is concentrated in the second miniband, the oscillator forces of electron resonance transitions in Eqs. (5.8) and (5.9) are determined by values k_0 and k_{-1}. These are included in Eqs. (5.8) and (5.9) if the minibands are overlapped, i. e.,$\varepsilon_0\eta^2 + 2\Delta > \varepsilon_{-1}$, and Fermi energy is concentrated in the overlap area $[\varepsilon_{-1}, \varepsilon_0\eta^2 + 2\Delta]$. Otherwise, the overlapping of minibands is absent. Then the maximum momentum of electrons k_0 in the completely occupied bottom miniband corresponds to Brillouin zone boundary π/d.

In the quantum limit, taking into account the spatial dispersion, the real part of conductivity depends on Fermi level position in the bottom miniband. If μ_0 is positioned in the bottom half of the miniband $(\varepsilon_0\eta^2 < \mu_0 < \varepsilon_0\eta^2 + \Delta$, $q < \pi/2d)$ from Eq. (5.6) we obtain

$$\mathrm{Re}\,\sigma_{zz} = \frac{e^2 (k^-)^2}{2\pi m_*^2 ad\omega}\left[4\Delta^2 \sin^2\frac{qd}{2} - \left(\omega - \Omega_+\right)^2\right]^{-1/2},$$

where

$$k^- = \frac{1}{d}\arcsin\frac{|\omega - \Omega_+|}{2\Delta\sin\dfrac{qd}{2}}, \quad \omega_- < \omega < \omega_+,$$

$$\omega_{\pm} = \Omega_+ \pm 2\Delta\sin\frac{qd}{2}\left(\alpha_0\sin\frac{qd}{2} + \sqrt{1-\alpha_0^2}\cos\frac{qd}{2}\right),$$

$$\alpha_0 = \frac{\varepsilon_0\eta^2 + \Delta - \mu_0}{\Delta}.$$

The real parts of other components of conductivity tensor are obtained from $\mathrm{Re}\,\sigma_{zz}$ using substitution of $(k^-)^2$ by $(\eta + m/2)^2/a^2$ in $\mathrm{Re}\,\sigma_{\varphi\varphi}$ and by $k^-(\eta + m/2)/a$ in $\mathrm{Re}\,\sigma_{\varphi z}$.

If the Fermi level is positioned in the upper half of the miniband $(\varepsilon_0\eta^2 + \Delta < \mu_0 < \varepsilon_0\eta^2 + 2\Delta$, $\pi/2d < q < \pi/d)$, we obtain

$$\mathrm{Re}\,\sigma_{zz} = \frac{e^2 (k^+)^2}{2\pi m_*^2 ad\omega}\left[4\Delta^2 \sin^2\frac{qd}{2} - \left(\omega - \Omega_+\right)^2\right]^{-1/2},$$

where

$$k^+ = \frac{\pi}{d} - k^-, \ \omega_- < \omega < \omega_+,$$

$$\omega_{\pm} = \Omega_+ \pm 2\Delta\sin\frac{qd}{2}\left(|\alpha_0|\sin\frac{qd}{2} + \sqrt{1-\alpha_0^2}\cos\frac{qd}{2}\right).$$

The real part of conductivity is nonzero in the area of Landau damping $[\omega_-, \omega_+]$ of electromagnetic waves in the tube.

In the quasi-classical case, the quantization of electron circular rotation can be neglected. That is possible under condition of $\varepsilon_0 \ll \mu_0$. Substituting the l summation by integrals in Eqs. (5.8) and (5.9), we obtain

$$\begin{aligned}\mathrm{Re}\,\sigma_{\varphi\varphi} &= \frac{e^2\omega}{8\pi m_*^2\left(a\varepsilon_0|m|\right)^3}\left(k_+ I_+ - k_- I_-\right),\\ \mathrm{Re}\,\sigma_{zz} &= \frac{e^2}{6\pi m_*^2 a\varepsilon_0|m|\omega}\left(k_+^3 I_+ - k_-^3 I_-\right),\end{aligned} \tag{5.12}$$

where

$$k_{\pm} = \frac{1}{d}\arccos\frac{\varepsilon_{\pm} + \Delta - \mu_0}{\Delta}, \ \varepsilon_{\pm} = \varepsilon_0\left(\frac{\omega}{2m\varepsilon_0} \mp \frac{m}{2}\right)^2,$$

$$I_{\pm}(m,\omega) = \Theta\left(\frac{\omega}{2m\varepsilon_0} \mp \frac{m}{2} + \sqrt{\frac{\mu_0}{\varepsilon_0}}\right)\Theta\left(\sqrt{\frac{\mu_0}{\varepsilon_0}} - \frac{\omega}{2m\varepsilon_0} \pm \frac{m}{2}\right),$$

and Θ is the Heaviside function. If $\omega > 0$ and $|m| < 2\sqrt{\mu_0/\varepsilon_0}$, the Eq. (5.12) become as follows

$$\mathrm{Re}\,\sigma_{\varphi\varphi} = \frac{e^2\omega}{8\pi m_*^2\left(a\varepsilon_0|m|\right)^3}\begin{cases}\left(k_+ - k_-\right), & 0 < \omega < \omega_-,\\ k_+, & \omega_- < \omega < \omega_+,\\ 0, & \omega > \omega_+,\end{cases} \tag{5.13}$$

$$\mathrm{Re}\,\sigma_{zz} = \frac{e^2}{6\pi m_*^2 a\varepsilon_0|m|\omega}\begin{cases}\left(k_+^3 - k_-^3\right), & 0 < \omega < \omega_-,\\ k_+^3, & \omega_- < \omega < \omega_+,\\ 0, & \omega > \omega_+,\end{cases} \tag{5.14}$$

where $\omega_{\pm} = 2\varepsilon_0|m|\sqrt{\mu_0/\varepsilon_0} \pm \varepsilon_0 m^2$. Equations (5.13) and (5.14) are

$$\mathrm{Re}\,\sigma_{\varphi\varphi} = \frac{e^2}{8\pi m_*^2\varepsilon_0^2\left(a|m|\right)^3 d}G_a,$$

$$\mathrm{Re}\,\sigma_{zz} = \frac{e^2}{6\pi m_*^2\varepsilon_0^2 a|m|d^3}G_b,$$

where

$$G_a(x)\begin{cases} x\left[\arccos\dfrac{\varepsilon_0\left(x-(\mu_0/\varepsilon_0)\right)^2}{4m^2\Delta}-\arccos\dfrac{\varepsilon_0\left(x+\mu_0/\varepsilon_0\right)^2}{4m^2\Delta}\right], & 0<x<x_-,\\ x\arccos\dfrac{\varepsilon_0\left(x-\mu_0/\varepsilon_0\right)^2}{4m^2\Delta}, & x_-<x<x_+,\\ 0, & x>x_+, \end{cases}$$

$$G_b(x)\begin{cases} \dfrac{1}{x}\left[\left(\arccos\dfrac{\varepsilon_0\left(x-(\mu_0/\varepsilon_0)\right)^2}{4m^2\Delta}\right)^3-\left(\arccos\dfrac{\varepsilon_0\left(x+(\mu_0/\varepsilon_0)\right)^2}{4m^2\Delta}\right)^3\right], & 0<x<x_-,\\ \dfrac{1}{x}\left(\arccos\dfrac{\varepsilon_0\left(x-(\mu_0/\varepsilon_0)\right)^2}{4m^2\Delta}\right)^3, & x_-<x<x_+,\\ 0, & x>x_+, \end{cases}$$

$x=\omega/\varepsilon_0$, $x_\pm=\omega_\pm/\varepsilon_0$. The value $(\mu_0/\varepsilon_0)^{1/2}$ in $\omega_\pm$ is equal to the classical angular moment ak_F of Fermi electron in the circular orbit (k_F is Fermi momentum). In Fig. 4 the dependences of G_a [Fig. 4 (a)], and G_b [Fig. 4 (b)] functions on x are shown for parameters $m=10$, $\mu_0/\varepsilon_0=\Delta/\varepsilon_0=100$ typical for semiconductor superlattices.

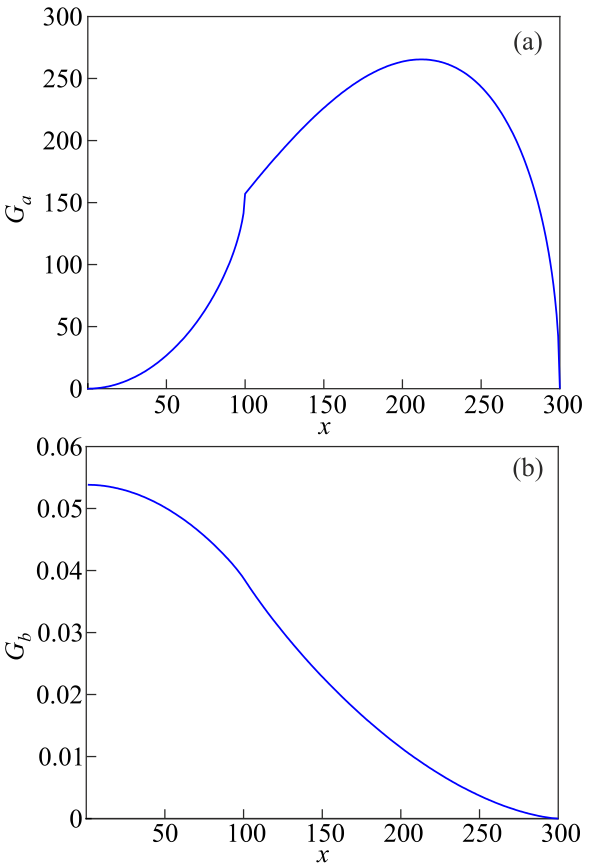

Fig. 4. The real part of conductivity (5.13) and (5.14) depending on frequency for values of parameters referred in the text under condition of $|m|<2\sqrt{\mu_0/\varepsilon_0}$.

At $|m|>2\sqrt{\mu_0/\varepsilon_0}$ we obtained

$$\mathrm{Re}\,\sigma_{\varphi\varphi}=\frac{e^2\omega}{8\pi m_*^2\left(a\varepsilon_0|m|\right)^3}\begin{cases}0, & 0<\omega<\omega_-,\\ k_+, & \omega_-<\omega<\omega_+,\\ 0, & \omega>\omega_+,\end{cases}\quad(5.15)$$

$$\mathrm{Re}\,\sigma_{zz}=\frac{e^2}{6\pi m_*^2 a\varepsilon_0|m|\omega}\begin{cases}0, & 0<\omega<\omega_-,\\ k_+^3, & \omega_-<\omega<\omega_+,\\ 0, & \omega>\omega_+,\end{cases}\quad(5.16)$$

where now $\omega_\pm=\pm 2\varepsilon_0|m|\sqrt{\mu_0/\varepsilon_0}+\varepsilon_0 m^2$. Functions (5.15) and (5.16) are represented as

$$\mathrm{Re}\,\sigma_{\varphi\varphi}=\frac{e^2}{8\pi m_*^2\varepsilon_0^2\left(a|m|\right)^3 d}F_a,$$

$$\mathrm{Re}\,\sigma_{zz}=\frac{e^2}{6\pi m_*^2\varepsilon_0^2 a|m|d^3}F_b,$$

where

$$F_a(x)=x\arccos\frac{\varepsilon_0\left(x-m^2\right)^2}{4m^2\Delta},\quad x_-<x<x_+,$$

$$F_b(x)=\frac{1}{x}\left[\arccos\frac{\varepsilon_0\left(x-m^2\right)^2}{4m^2\Delta}\right]^3,\quad x_-<x<x_+,$$

$x=\omega/\varepsilon_0$, $x_\pm=\omega_\pm/\varepsilon_0$. In Fig. 5 the dependences of F_a [Fig. 5 (a)], and [Fig. 5 (b)] F_b functions on x are shown for parameters $m=5$, $\mu_0/\varepsilon_0=\Delta/\varepsilon_0=4$ under condition of $|m|>2\sqrt{\mu_0/\varepsilon_0}$.

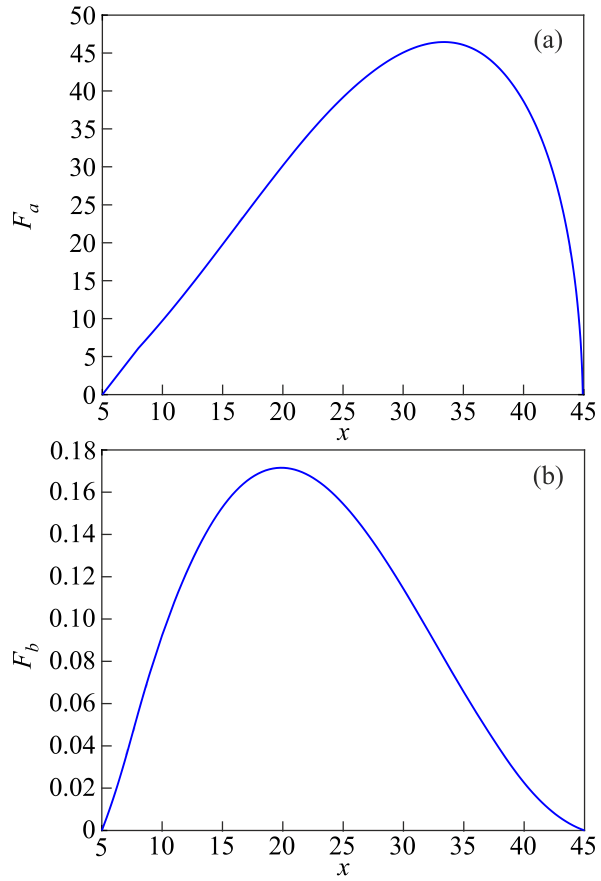

Fig. 5. The real part of conductivity from Eqs. (5.15) and (5.16) depending on frequency for values of parameters referred in the text under condition of $|m| > 2\sqrt{\mu_0/\varepsilon_0}$.

As the real part of conductivity is connected with electromagnetic field energy absorbed by electrons, the Eqs. (5.13)–(5.16) determine the boundaries of Landau damping for waves with positive and negative helicity. These boundaries are parabolas in the "angular moment – frequency" plane. The real part of the conductivity determines the damping decrement of electromagnetic waves on the tube. High-frequency asymptotics of the conductivity imaginary part at $\omega \gg \Omega_{\pm}$ are

$$\mathrm{Im}\,\sigma_{\varphi\varphi} = \frac{e^2 n}{m_*\omega} + \frac{2e^2 m}{\pi^2 m_*^2 a^3 \omega^2}\sum_l k_l\left(l+\eta\right), \qquad (5.17)$$

$$\mathrm{Im}\,\sigma_{zz} = \frac{e^2 n}{m_*\omega} + \frac{2e^2\varepsilon_0 m^2}{3\pi^2 m_*^2 a\omega^3}\sum_l k_l^3. \qquad (5.18)$$

If $\varepsilon_0 \ll \mu_0$, the sums by l included in Eqs. (5.17) and (5.18) are calculated by Poisson formula. Then the Eqs. (5.17) and (5.18) for components contain monotonic (σ^{mon}) addends and oscillating (σ^{osc}) ones. These depend on the ratio of Fermi energy to the miniband width. When $\omega \gg \Omega_{\pm}$, $\varepsilon_0 \ll \mu_0$ and $\mu_0 < 2\Delta$ after integration by parts and replacing the integration variable, the oscillating part of the sum $J = \sum_l k_l(l+\eta)$ in formula (5.17) is equal to

$$J_{\mathrm{osc}} = -\frac{4}{\pi d}\sqrt{\frac{\mu}{\varepsilon_0}}\sum_{r=1}^{\infty}\frac{1}{r}\sin 2\pi r\eta\int_0^1 dy\,\frac{y^2\cos\left(2\pi r\sqrt{\frac{\mu}{\varepsilon_0}}y\right)}{\sqrt{\left(1-y^2\right)\left(y^2+\alpha^2\right)}},$$

$$\alpha = \sqrt{(2\Delta-\mu)/\mu}\,.$$

Asymptotic of this integral under $\mu_0 \gg \varepsilon_0$ as is known [80]. As a result, the imaginary part of the transverse conductivity (5.17) is equal

$$\mathrm{Im}\,\sigma_{\varphi\varphi} = \frac{e^2 n}{m_*\omega} - \frac{2^{3/2}e^2 m}{\pi^3 m_*^2 a^3 d\omega^2}\left(\frac{\mu}{\varepsilon_0}\right)^{1/4}\left(\frac{\mu}{\Delta}\right)^{1/2}\times$$
$$\times\sum_{r=1}^{\infty}\frac{\sin 2\pi r\eta}{r^{3/2}}\cos\left(2\pi r\sqrt{\frac{\mu}{\varepsilon_0}}-\frac{\pi}{4}\right). \qquad (5.19)$$

In the case of $\mu_0 > 2\Delta$ we obtain,

$$\mathrm{Im}\,\sigma_{\varphi\varphi} = \frac{e^2 n}{m_*\omega} - \frac{2^{3/2}e^2 m}{\pi^3 m_*^2 a^3 d\omega^2}\left(\frac{\mu}{\varepsilon_0}\right)^{1/4}\left(\frac{\mu}{\Delta}\right)^{1/2}\sum_{r=1}^{\infty}\frac{\sin 2\pi r\eta}{r^{3/2}}\times$$
$$\times\left[\cos\left(2\pi r\sqrt{\frac{\mu}{\varepsilon_0}}-\frac{\pi}{4}\right)+\left(\frac{\mu-2\Delta}{\mu}\right)^{3/4}\cos\left(2\pi r\sqrt{\frac{\mu-2\Delta}{\varepsilon_0}}+\frac{\pi}{4}\right)\right]. \qquad (5.20)$$

The Eqs. (5.19) and (5.20) undergoes Aharonov–Bohm oscillations under variation of magnetic flux through the tube cross-section. The oscillation period is equal to the flux quantum Φ_0. Also the oscillations looking like de Haas–van Alphen ones exist. They are caused by transition of root singularities of electron density of states at the miniband boundaries through Fermi boundary due to the tube radius variation or changing the electron density. The latter is related with Fermi energy as follows

$$\mu_0 = \begin{cases} \dfrac{\pi}{2}dn\sqrt{\dfrac{\Delta}{m_*}}, & \mu \ll 2\Delta, \\ \dfrac{1}{8m_*}(\pi dn)^2, & \mu \gg 2\Delta. \end{cases}$$

Analyzing the dependence of oscillations (5.19) on $(adn)^{1/2}$ we obtain the period $\tau = (\pi a\sqrt{m_*\Delta})^{-1/2}$.

If $\mu_0 < 2\Delta$, only the miniband bottom boundaries ε_l pass through Fermi boundary when the tube parameters change. As a result, in Eq. (5.19) the base frequency of oscillations is present only. The second addend in Eq. (5.20) exists because at $\mu_0 > 2\Delta$ not only miniband ε_l bottom boundaries transverse Fermi level but the upper ones $\varepsilon_l + 2\Delta$ as well. Existence of two oscillation frequencies in Eq. (5.20) causes the beats in the plot of conductivity versus the tube parameters. They are similar to the beats of plasma and spin waves spectra in the tube [26, 27]. If $\Delta \ll \mu_0$ the

relative difference of conductivity oscillation frequencies and amplitudes in Eq. (5.20) is of the order of Δ/μ_0. As this parameter increases, the beats turn into weak modulations and disappear at $\mu_0 < 2\Delta$. The sum by l in longitudinal conductivity (5.18) is calculated by Poisson formula as well. Consequently, the conductivity contains monotonic and oscillating components. At $\mu_0 > 2\Delta$ they are equals

$$\mathrm{Im}\,\sigma_{zz}^{\mathrm{mon}} = \frac{e^2 n}{m_* \omega} + \frac{2e^2\varepsilon_0 m^2}{3\pi^2 m_*^2 a\omega^3 d^3} J_{\mathrm{mon}}, \qquad (5.21)$$

$$\mathrm{Im}\,\sigma_{zz}^{\mathrm{osc}} = \frac{2e^2\varepsilon_0 m^2}{3\pi^2 m_*^2 a\omega^3 d^3} \sum_{r=1}^{\infty} \cos 2\pi r\eta \cdot J_{\mathrm{osc}}^r, \qquad (5.22)$$

where

$$J_{\mathrm{mon}}(b) = 2\int\limits_{\sqrt{b^2-2c^2}}^{b} dx \left(\arccos\frac{x^2-b^2+c^2}{c^2}\right)^3, \qquad (5.23)$$

$$J_{\mathrm{osc}}^r(b) = 4\int\limits_{\sqrt{b^2-2c^2}}^{b} dx \cos(2\pi r x)\left(\arccos\frac{x^2-b^2+c^2}{c^2}\right)^3,$$

$$b = (\mu/\varepsilon_0)^{1/2}, \quad c^2 = \Delta/\varepsilon_0. \qquad (5.24)$$

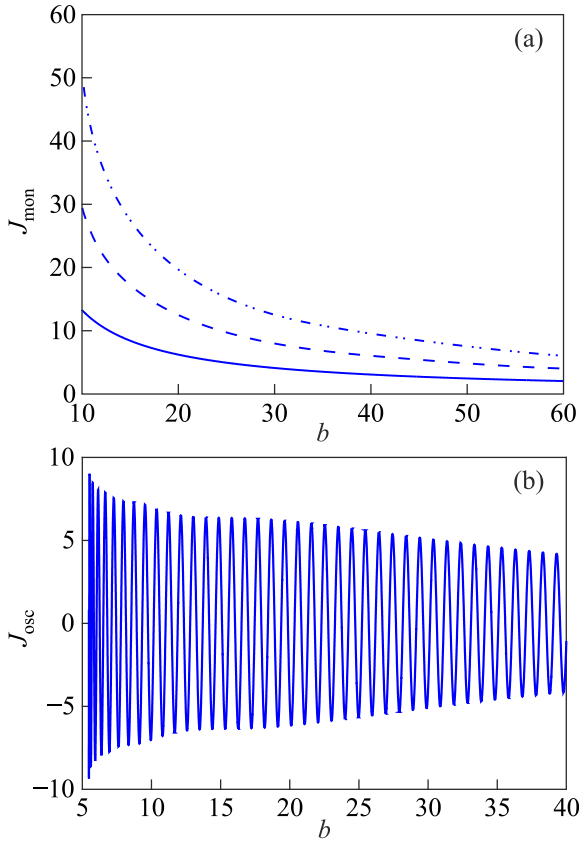

Fig. 6. Monotonic (a) and oscillating (b) components of longitudinal conductivity (5.21) and (5.22) at $\mu_0 > 2\Delta$ as the functions of $(\mu_0/\varepsilon_0)^{1/2}$ for parameter values referred in the text.

The integrals (5.23) and (5.24) are not calculated exactly. In Fig. 6 (a), the dependence $J_{\mathrm{mon}}(b)$ calculated numerically is shown. Solid-, dotted-, and chain-line curves correspond to $c^2 = 10, 20, 30$, respectively. The $J_{\mathrm{osc}}(b)$ dependence at $r = 1$ and $c^2 = 15$ is shown in Fig. 6 (b).

In accordance with formulas (5.21)–(5.24) the monotonic part of the conductivity and the amplitude of the oscillating part decrease with frequency ω_n increases. Figue 6 (b) shows the weak modulations are caused by the beats.

The imaginary part of the transverse conductivity (5.19) and (5.20) behaves similarly. It is includes into the dispersion equation for the electromagnetic waves spectrum. The beats and oscillations obtained here there exist only in the quasiclassical case. Their reasons were described above. The ratio of the oscillation amplitude of the transverse conductivity (5.19) to the amplitude of the oscillation in the absence of the superlattice [58] is of order $a/d(\varepsilon_0/\Delta)^{1/2}$. The longitudinal conductivity oscillations of de Haas–van Alphen type exist also in the absence of magnetic field.

5.2. Magnetic susceptibility

Within the framework of random phase approximation [78, 87, 88], circular components of the tensor of dynamical spin susceptibility of an electron gas with the spectrum (3.2) on the tube surface are [89–91]

$$\chi_{\pm}(m,q,\omega) = \chi_{\pm}^0(m,q,\omega)\left[1 - \frac{g}{2\mu_B^2}\chi_{\pm}^0(m,q,\omega)\right]^{-1}, \qquad (5.25)$$

where

$$\chi_{\pm}^0(m,q,\omega) = \frac{2\mu_B^2}{S}\sum_{lk}\frac{f(\varepsilon_{(l+m)(k+q)\mp}) - f(\varepsilon_{lk\pm})}{\omega + \varepsilon_{lk\pm} - \varepsilon_{(l+m)(k+q)\mp} + i0} \qquad (5.26)$$

is the susceptibility of the ideal electron gas with spectrum (3.2), $\chi_{\pm} = \chi_{xx} \pm i\chi_{yx}$, m, q and ω are, respectively, angular moment, moment and frequency of the spin wave.

The real and imaginary parts of the component χ_-^0 (5.26) of electron degenerated gas are

$$\mathrm{Re}\,\chi_-^0(m,q,\omega) = \frac{\mu_B^2}{4\pi^2 ad\Delta\sin\frac{qd}{2}} \times$$

$$\times\sum_l\left[P\int\limits_{\left(-k_l^+ - \frac{q}{2}\right)d}^{\left(k_l^+ - \frac{q}{2}\right)d} dx\cdot(C_- - \sin x)^{-1} - \right. \qquad (5.27)$$

$$\left. -P\int\limits_{\left(-k_l^- + \frac{q}{2}\right)d}^{\left(k_l^- + \frac{q}{2}\right)d} dx\cdot(C_+ - \sin x)^{-1}\right],$$

$$\mathrm{Im}\,\chi_-^0(m,q,\omega)=\frac{\mu_B^2}{4\pi ad\Delta\left|\sin\frac{qd}{2}\right|}\times$$

$$\times\sum_l\left[\int\limits_{\left(-k_l^-+\frac{q}{2}\right)d}^{\left(k_l^-+\frac{q}{2}\right)d}dx\cdot\delta(\sin x-C_+)-\int\limits_{\left(-k_l^++\frac{q}{2}\right)d}^{\left(k_l^+-\frac{q}{2}\right)d}dx\cdot\delta(\sin x-C_-)\right], \tag{5.28}$$

where

$$k_l^\pm=\frac{1}{d}\arccos\frac{\varepsilon_l^\pm+\Delta-\mu_0}{\Delta}$$

is the maximum moment of electrons in the miniband with $(l,\sigma=\pm)$ number,

$$C_\pm=\frac{\omega-\Omega_\pm}{2\Delta\sin\frac{qd}{2}},\quad \Omega_\pm=\varepsilon_0 m\left[2(l+\eta)\pm m\right]+\Omega \tag{5.29}$$

are frequencies of vertical transitions of electrons between miniband boundaries $[\varepsilon_l^\pm,\varepsilon_l^\pm+2\Delta]$ (where $\varepsilon_l^\pm=\varepsilon_0(l+\eta)^2+$ $+\sigma\mu_B B+gn_{-\sigma}$) with spin-flip transition $-\to+$ under action of an alternating field. Sum over l in (5.27) and (5.28) is limited by the condition $\left|\varepsilon_l^\pm+\Delta-\mu_0\right|<\Delta$ which means that Fermi energy is in the miniband $(l,\sigma=\pm)$.

6. Collective excitations on a tube with a superlattice

6.1. Plasmons

In the framework of the hydrodynamic approach, using the continuity equation for electron liquid and Poisson equation for electrical potential, the authors [65, 66] have obtained the dispersion equation for the spectrum of surface plasma waves on the tube:

$$\omega=4\pi a\left[\frac{m^2}{a^2}\mathrm{Im}\,\sigma_{\varphi\varphi}(m,\omega)+q^2\,\mathrm{Im}\,\sigma_{zz}(m,\omega)\right]\times \tag{6.1}$$
$$\times I_m(qa)K_m(qa)$$

where m is the projection of the plasmon angular moment on the tube axis z; $\sigma_{\varphi\varphi}$ and σ_{zz} are components of electron gas dynamical conductivity in absentia of spatial dispersion ($q\upsilon_0\ll\omega$, υ_0 is the Fermi velocity) in cylindrical coordinates φ,z; I_m and K_m are modified Bessel functions.

The Eq. (6.1) is true also for the tube with a superlattice. Substituting Drude expression for conductivity $ie^2n/m_*\omega$ into Eq. (6.1), we obtained the known spectrum for intraband ($m=0$) and interband ($m\neq0$) plasmons [65–67]:

$$\Omega_{mq}^2=\frac{4\pi e^2an}{m_*}\left[\frac{m^2}{a^2}+q^2\right]I_m(qa)K_m(qa). \tag{6.2}$$

The Eq. (6.2) does not take into account the interband current caused by quantum transitions of electrons in the wave field between the minibands. Taking that into account, the transverse component of dynamical conductivity tensor for electron gas on the tube is

$$\sigma_{\varphi\varphi}=\mathrm{i}\frac{e^2n}{m_*\omega}+\mathrm{i}\frac{2e^2}{m_*^2a^2\omega S}\sum_{lk}f(\varepsilon_{lk})\times$$
$$\times\left[\left(l+\frac{m}{2}\right)^2(\omega-\Omega_++\mathrm{i}0)^{-1}-\left(l-\frac{m}{2}\right)^2(\omega-\Omega_-+\mathrm{i}0)^{-1}\right], \tag{6.3}$$

where $\Omega_\pm=\varepsilon_0 m(2l\pm m)$ are frequencies of direct transitions of electrons between the minibands. The longitudinal conductivity σ_{zz} is obtained from (6.3) using substitution of $a^{-2}\left(l\pm\frac{m}{2}\right)^2$ by k^2 and $\sigma_{\varphi z}=\sigma_{z\varphi}=0$. In Eq. (6.3) we apply the electron energy on the surface of the semiconductor nanotube with a superlattice [26, 74]: $\varepsilon_{lk}=\varepsilon_0 l^2+$ $+\Delta(1-\cos kd)$. The imaginary part of the interband conductivity has resonance singularities at frequencies $\Omega_\pm$. The Landau attenuation is concentrated in narrow bands $\delta\omega\sim\Delta qd$ near these frequencies [27].

In formulas for conductivity, we restrict ourselves to the quantum limit where electrons in the degenerated gas occupy partially only the lower miniband $l=0$ with width 2Δ and their density does not exceed $1/\pi ad$. In this case, the solution of Eq. (6.1) is defined by the parameter $\alpha_m=3m^2/4(ak_0)^2$. That is connected with forces of oscillators for resonance transitions $0\to m$ of electrons between the minibands. Here

$$k_0=\frac{1}{d}\arccos\frac{\Delta-\mu_0}{\Delta}$$

is the maximum momentum of an electron in the miniband with $l=0$.

If $\alpha_m<1$, there exists a series of branches in the plasmon spectrum

$$\omega_{mq}^2=\frac{1}{2}\left\{\omega_m^2+\Omega_{mq}^2+\left[\left(\omega_m^2+\Omega_{mq}^2\right)^2+\right.\right.$$
$$\left.\left.+\frac{16}{3}\left(\frac{a}{m}\right)^4\omega_m^2\Omega_{mq}^2(1-\alpha_m)(qk_0)^2\left(1+\frac{q^2a^2}{m^2}\right)^{-1}\right]^{1/2}\right\}, \tag{6.4}$$

where $\omega_m=\varepsilon_0 m^2$ are frequencies of electron single-particle transitions $0\to m$. Figure 7 shows the frequency of the wave (6.4) $\omega'_{1q}=\omega_{1q}/\Omega_{10}$ (solid line) and wave (6.2) $\Omega'_{1q}=\Omega_{1q}/\Omega_{10}$ (dashed curve) as a function of $x=qa$ for $m=1$ and $\alpha_1=0.75$. Here $\Omega_{10}=(2\pi e^2n/m_*a)^{1/2}$ is the limiting frequency for the wave with the spectrum (6.2). Parameter values $m_*=0.64\cdot10^{-28}$ g (GaAs), $a=10^{-7}$ cm, $k_0a=1$ are used. Under the condition $\alpha_1<1$ the Fermi level lies in the upper half of the miniband. If $\alpha_m>1$, then two branches are connected with each $0\to m$ transition:

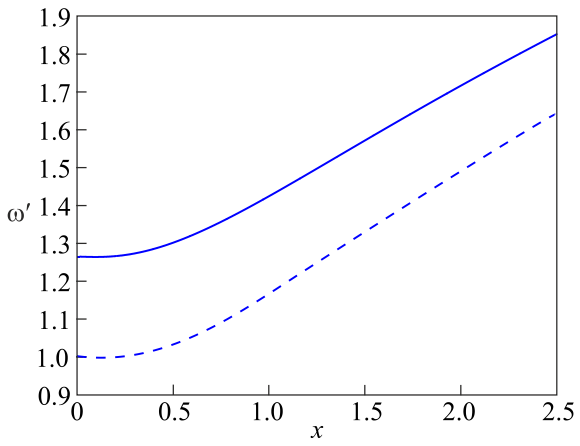

Fig. 7. The dispersion curves of waves with the spectrum (6.4) (solid line) and with the spectrum (6.2) (dashed line) under $m=1$, $\alpha_1<1$ are shown. Parameter values are given in the text.

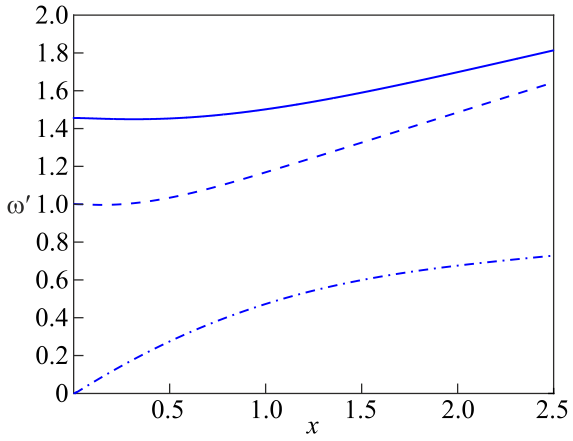

Fig. 8. The dispersion curves of waves with the spectrum (6.5) (solid and dash-dotted curves) and with the spectrum (6.2) (dashed line) under $m=1$, $\alpha_1>1$ are shown. The parameters values are given in the text.

$$\omega_{\pm}^2(m,q)=\frac{1}{2}\left\{\omega_m^2+\Omega_{mq}^2\pm\left[\left(\omega_m^2+\Omega_{mq}^2\right)^2-\right.\right.$$
$$\left.\left.-\frac{16}{3}\left(\frac{a}{m}\right)^4\omega_m^2\Omega_{mq}^2\left(\alpha_m-1\right)\left(qk_0\right)^2\left(1+\frac{q^2a^2}{m^2}\right)^{-1}\right]^{1/2}\right\}. \tag{6.5}$$

Figure 8 shows the dependence of the wave frequencies (6.5) $\omega'_{\pm}(1,q)=\omega_{\pm}(1,q)/\Omega_{10}$ (solid and dash-dotted curves) and wave (6.2) $\Omega'_{1q}=\Omega_{1q}/\Omega_{10}$ (dashed curve) as a function of $x=qa$ under $m=1$ and $\alpha_1=3$. The above mentioned values of m_*, a, and $k_0a=0.5$ were used. In this case the Fermi level lies in the lower half of the miniband. The branches (6.4) and ω_+ (6.5) are positioned above ω_m, and the branches ω_- (6.5) are below ω_m.

In the limit of long waves ($qa\ll1$) and at $\alpha_m<1$ from Eq. (6.4) we obtain

$$\omega_{1q}^2=\omega_{10}^2\left[1+\frac{1}{2}\frac{\Omega_{10}^2}{\omega_1^2+\Omega_{10}^2}\left(qa\right)^2\ln qa+\right.$$
$$\left.+\frac{4}{3}\frac{\omega_1^2\Omega_{10}^2}{\left(\omega_1^2+\Omega_{10}^2\right)^2}\left(1-\alpha_1\right)\left(k_0a\right)^2\left(qa\right)^2\right], \tag{6.6}$$

$$\omega_{mq}^2=\omega_{m0}^2\left[1+\frac{\Omega_{m0}^2}{\omega_m^2+\Omega_{m0}^2}\frac{m^2-2}{2m^2\left(m^2-1\right)}\left(qa\right)^2+\right.$$
$$\left.+\frac{4}{3m^4}\frac{\omega_m^2\Omega_{m0}^2}{\left(\omega_m^2+\Omega_{m0}^2\right)^2}\left(1-\alpha_m\right)\left(k_0a\right)^2\left(qa\right)^2\right],\quad m=\pm2,\pm3,\ldots \tag{6.7}$$

The critical frequencies of waves with spectra (6.6) and (6.7) are

$$\omega_{m0}^2=\omega_m^2+\Omega_{m0}^2=\varepsilon_0^2m^4+\frac{2e^2k_0\left|m\right|}{\pi m_*a^2}. \tag{6.8}$$

The frequency depolarization shift in Eq. (6.8) contains the period and the amplitude of the superlattice modulating potential. At $\alpha_m>1$ the expressions (6.6) and (6.7) are true for the upper branch ω_+. The bottom branch ω_- has the sound spectrum $\omega_-(m,q)=c_mq$, where

$$c_m^2=\frac{4a^2}{3m^4}\left(k_0a\right)^2\frac{\omega_m^2\Omega_{m0}^2}{\omega_{m0}^2}\left(\alpha_m-1\right). \tag{6.9}$$

Optical ω_+ and acoustic ω_- branches are connected with in-phase and anti-phase density oscillations of electrons which participate in longitudinal and transversal motion on the tube.

6.2. Spin waves

In the random-phase approximation, the dispersion equation for the spectrum of transverse spin waves on a tube with a superlattice in the magnetic field has the form [34]

$$1-\frac{g}{2\mu_B^2}\chi_{\pm}^0\left(m,q,\omega\right)=0. \tag{6.10}$$

Components $\chi_{\pm}$ correspond to spin transversal waves with positive (–) and negative (+) helicity. The plus (minus) sign in $\chi_{\pm}$ corresponds to transverse Landau–Silin spin waves [69–72] with a negative (positive) chirality. The solution of Eq. (6.10) for a degenerate electron gas depends on the position of the Fermi level μ_0. If the electron density n satisfies the inequality

$$n<\frac{1}{2\pi^2a}\left(k_0^-+k_0^+\right), \tag{6.11}$$

the Fermi level occurs in the miniband overlapping region in Fig. 1. Inequality (6.11) involves

$$k_0^{\pm}=\frac{1}{d}\arccos\frac{\varepsilon_0^{\pm}+\Delta-\mu_0}{\Delta},$$

which is the maximum electron momentum in the miniband $0^{\pm}$. If the minibands do not overlap and the level μ_0 is situated in the second miniband then k_0^- in Eq. (6.11) should be replaced by π/d.

The graphical analysis of Eq. (6.10) in the case $\varepsilon_0^+ < \mu_0 < \varepsilon_0^- + 2\Delta$ indicates that each m value, i. e., each spin-flip $-\to+$ electron transition $0^- \to m^+$ between the minibands $l = 0$ and $l = m$ corresponds to two branches of the magnon spectrum with a positive chirality. These branches are situated between the frequencies of single-electron transitions between the minibands

$$\Omega_{\pm} = \varepsilon_0 m\left[2\eta \pm m\right] + \Omega.$$

In the long-wavelength limit $\left(2\Delta\left|\sin\frac{qd}{2}\right| \ll \left|\omega - \Omega_{\pm}\right|\right)$, the magnon spectrum with a positive chirality reads

$$\omega_{\pm}(q) = \omega_{\pm}^0 + \alpha_{\pm}\sin^2\frac{qd}{2}, \qquad (6.12)$$

where

$$\omega_{\pm}^0 = \frac{1}{2}\left[\Omega_+ + \Omega_- - \upsilon\left(k_0^- - k_0^+\right)\right] \pm$$
$$\pm\frac{1}{2}\left[\left(\Omega_+ - \Omega_-\right)^2 - 2\upsilon\left(k_0^- - k_0^+\right)\left(\Omega_+ + \Omega_-\right) + \right. \qquad (6.13)$$
$$\left. + \upsilon^2\left(k_0^- - k_0^+\right) - 4\upsilon\left(k_0^+\Omega_+ - k_0^-\Omega_-\right)\right]^{1/2}$$

are the limiting frequencies of the modes,

$$\upsilon = \frac{g}{2\pi^2 a},$$

$$\alpha_{\pm} = 2\Delta\frac{\sin k_0^+ d\left(\omega_{\pm}^0 - \Omega_+\right)^2 + \sin k_0^- d\left(\omega_{\pm}^0 - \Omega_-\right)^2}{k_0^+ d\left(\omega_{\pm}^0 - \Omega_+\right)^2 - k_0^- d\left(\omega_{\pm}^0 - \Omega_-\right)^2}. \qquad (6.14)$$

If the minibands 0^- and 0^+ do not overlap, k_0^- in Eqs. (6.13) and (6.14) must be replaced by π/d. The spectrum of negative-chirality spin waves can be found from Eqs. (6.13) and (6.14) by exchanging the spin indices $-\leftrightarrow+$ and a sign change of Ω.

In the case of weak electron-electron interaction $\upsilon \ll d\Omega_{\pm}$, we find from Eqs. (6.13) and (6.14)

$$\omega_{\pm}^0 = \Omega_{\pm} - \upsilon k_0^{\mp}, \qquad (6.15)$$

$$\alpha_{\pm} = \mp 2\Delta\frac{\sin k_0^{\mp} d}{k_0^{\mp} d}, \qquad (6.16)$$

where $\upsilon k_0^{\mp}$ is the depolarization frequency shift. The upper (lower) branch ω_+ (ω_-) of the magnon spectrum has a negative (positive) chirality. Collisionless damping of spin waves is given by the imaginary part of susceptibility (5.26). In the case of a degenerate electron gas, it is

$$\operatorname{Im}\chi_- = \frac{\mu_B^2}{2\pi a d}\sum_l\left[4\Delta^2\sin^2\frac{qd}{2} - \left(\omega - \Omega_+\right)^2\right]^{-1/2}, \qquad (6.17)$$

where frequency is in the interval

$$\Omega_+ - 2\Delta\sin\frac{qd}{2} < \omega < \Omega_+ + 2\Delta\sin\frac{qd}{2},$$

$$\operatorname{Im}\chi_- = -\frac{\mu_B^2}{2\pi a d}\sum_l\left[4\Delta^2\sin^2\frac{qd}{2} - \left(\omega - \Omega_-\right)^2\right]^{-1/2}, \qquad (6.18)$$

where frequency is in the interval

$$\Omega_- - 2\Delta\sin\frac{qd}{2} < \omega < \Omega_- + 2\Delta\sin\frac{qd}{2}.$$

The Landau damping of spin waves is nonzero in the Stoner sectors of the $q-\omega$ plane bounded by the curves $\omega_{\pm} = \Omega_{\pm} \pm 2\Delta\sin\frac{qd}{2}$. Dispersion curves (6.12) are situated outside the Stoner sectors, i. e., the spin waves considered in this Subsection are undamped. To observe the effects associated with these modes the distances between the edges $\upsilon k_0^{\pm} = 2\pi^2 a\upsilon n_{\pm}$ of the Stoner sector and the limiting frequencies must exceed both the thermal and impurity broadening of the electron energy levels.

Conclusion

Superlattice at the surface of a nanotube has a significant impact on its properties. It can be obtained by embedding fullerenes or other additives to the nanotube or when the nanotube is attached to a substrate for charge exchange [47]. In the absence of a superlattice, the tube spectrum in a longitudinal magnetic field is a collection of one-dimensional subbands located next to each other and having nonequidistant boundaries [22, 26, 27, 34, 86, 89]. Periodic modulating potential artificially created at the surface of the tube converts the spectrum into a system of minibands, the widths of which are determined by the amplitude of the modulating potential [22]. In a longitudinal magnetic field its amplitude and period depend on the magnetic field strength. Energy gaps separating the minibands have widths defined by the ratio of the miniband width to the magnitude of the rotational quantum and depend on magnetic field strength [26, 27]. Density of electronic states has a root singularity at miniband borders [22]. As the radius of the tube increases, the minibands overlap resulting in a continuous spectrum [22].

In this review, the density of states, chemical potential, energy, and heat capacity of a degenerate and non-degenerate electron gas at the surface of a nanotube with metallic conductivity character in a longitudinal magnetic field have been presented [22]. We show that abovementioned thermodynamic values include monotonic and oscillating components. In agreement with Pauli principle monotonic heat capacity component of a degenerate electron gas is

proportional to the temperature [22]. Heat capacity displays de Haas–van Alphen type oscillations due to the passage of state density root singularity through the Fermi boundary with a change in electron density [22]. These oscillations persist in the absence of a magnetic field. Heat capacity also displays Aharonov–Bohm type oscillations when magnetic field flux through cross-sectional of the tube is varied. Heat capacity studies allow observation of the transition of modulating potential from the localized gaps mode to the mode of free motion along the tube [22].

The obtained in the present review formulas for the conductivity tensor components may be applied for studying electromagnetic wave propagation in nanotubes with superlattices based on Al_xGa_{1-x}/GaAS, InGaAs/GaAs, InAs/GaAs, GeSi/Si heterojunctions and in carbon nanotubes in the regime of metallic conductivity. The real part of conductivity determines the wave energy absorbed by electrons [24]. In the degenerated electron gas, this is nonzero in the areas of Landau collisionless damping [24]. Knowing the positions of transparency windows for the waves, it is possible to improve the waveguide characteristics of nanotubes [21]. The imaginary part of conductivity is included into the dispersion equation for electromagnetic wave spectrum [32, 65–67]. This has the resonance singularities at frequencies of electron direct transitions between minibands. Usually, near these frequencies there exist new branches in the wave spectrum and related band transparency. Observation of conductivity oscillations of de Haas–van Alphen type allows determining the electron effective mass, Fermi momentum, rotational quantum and superlattice parameters d and Δ [24]. These values are included in the oscillation amplitude and period expressions. Revealing the instant of appearing the beats under variation of the nanotube parameters gives the opportunity to obtain the ratio of Fermi energy to miniband width.

In the framework of the hydrodynamic approach, the plasma waves on the surface of a nanotube with a longitudinal superlattice were discussed [32]. Not only longitudinal electron current but also transversal one has been taken into consideration. It has been shown that both optical and acoustical plasmons could propagate along the tube with one sort of carrier [32]. The results of this review can be used in studying the magnetic scattering of neutrons by the spin magnetization current of conduction band electrons on a tube. The cross-sections of scattering by spin waves and Stoner excitations are of interest. This problem was solved earlier for a two-dimensional electron gas on a plane [73]. The curvature of a cylinder should manifest itself in additional features of the scattering cross-section. The electron-electron interaction constant, the amplitude, and period of the modulating potential can be found by measuring the depolarization frequency shift and group velocity of spin waves on a tube [31].

The authors are thankful to T. I. Rashba for help during the manuscript preparation.

1. I. M. Lifshitz, M. Ya. Azbel, and M. I. Kaganov, *The Electron Theory of Metals*, Nauka, Moscow (1971).
2. L. V. Keldysh, *Fiz. Tverd. Tela* **4**, 2265 (1962).
3. Zh. I. Alferov, Yu. V. Zhilyaev, and Yu. V. Shmartsev, *Sov. Phys. Semicond*. **5**, 174 (1971).
4. L. Esaki and R. Tsu, *IBM J. Dev.* **14**, 61 (1970).
5. L. Cheng and K. Plog, *Molecular Beam Epitaxy and Heterostructures,* Martinus Nijhoff, Dordrecht (1985).
6. M. I. Kaganov and I. L. Sklovskaya, *Fiz. Tverd. Tela*, **8**, 3480 (1966) [in Russian].
7. M. Kaganov, V. N. Lutskii, and D. V. Posvyanskh, *Fiz. Nizk. Temp*. **15**, 846 (1989) [*Sov. J. Low Temp. Phys.* **15**, 469 (1989)].
8. V. N. Lutskii, M. I. Kaganov, and A. Ya. Shik, *Zh. Eksp. Teor. Fiz.* **92**, 721 (1987).
9. L. Vendler and M. I. Kaganov, *Pis'ma Zh. Eksp. Teor. Fiz.* **44**, 345 (1986) [in Russian].
10. M. I. Kaganov, *Physics Through the Eyes of a Physicist, Moscow Center for Continuous Mathematical Education*, Moscow (2014), Part 2 [in Russian].
11. A. Ya. Shik, *Fiz. Tekh. Poluprovodn*. **8**, 1841 (1974) [in Russian].
12. K. Ploog and G. H. Dohler, *Adv. Phys.* **32**, 285 (1983).
13. A. P. Silin, *Usp. Fiz. Nauk* **147**, 485 (1985).
14. F. G. Bass and A. P. Tetervov, *Phys. Rep.* **140**, 237 (1986).
15. F. G. Bass, A. A. Bulgakov, and A. P. Tetervov, *Quality Properties of Conductors with Superlattices*, Nauka, Moscow (1989).
16. M. A. Herman, *Semiconductor Superlattices,* Akademie-Verlag, Berlin (1986).
17. N. A. Shulga, *Fundamentals of Mechanics of Layered Environment of Periodic Structure*, Naukova Dumka, Kiev (1981) [in Russian].
18. V. Dragunov, I. Neizvestnyi, and V. Gridchin, *Fundamentals of Nanoelectronics*, Logos, Moscow (2006).
19. A. M. Ermolaev and G. I. Rashba, *J. Phys.: Condens. Matter* **20**, 175212 (2008).
20. A. M. Ermolaev and G. I. Rashba, *Eur. Phys. J. B* **66**, 223 (2008).
21. P. N. Dyachkov, *Electronic properties and application of nanotubes*, Binom. Laboratory of Knowledge, Moscow (2012).
22. A. M. Ermolaev, G. I. Rashba, and M. A. Solyanik, *Fiz. Nizk. Temp.* **37**, 1033 (2011) [*Low Temp. Phys.* **37**, 824 (2011)].
23. A. M. Ermolaev and G. I. Rashba, *Bulletin KhNU named after V. N. Karazin, Ser. "Physics"* **1075**, 14 (2013).
24. A. M. Ermolaev, and G. I. Rashba, *Physica B* **451**, 20 (2014).
25. A. M. Ermolaev and G. I. Rashba, *Plasma Waves on the Surface of Superlattice Nanotube in Magnetic Field: International Anniversary Seminar* "*Modern Problems Of Solid State Physics*", *In Memory of Corresponding Member of The Academy of Sciences Of Ukraine E. A. Kaner*, Kharkiv (2011) [in Russian].
26. A. M. Ermolaev, G. I. Rashba, and M. A. Solyanik, *Fiz. Nizk. Temp.* **38**, 653 (2012) [*Low Temp. Phys.* **38**, 511 (2012)].

27. A. M. Ermolaev, G. I. Rashba, and M. A. Solyanik, *Fiz. Nizk. Temp.* **38**, 1209 (2012) [*Low Temp. Phys.* **38**, 957 (2012)].
28. A. M. Ermolaev, G. I. Rashba, and M. A. Solyanik, *Bulletin KhNU named after V. N. Karazin, Ser. "Physics"* **1019**, 10 (2012).
29. A. M. Ermolaev and G. I. Rashba, *Interband Current and Plasmons on the Surface of Nanotube with the Superlattice: International Conference "Physical Phenomena in Solids"*, Kharkiv (2013) [in Russian].
30. A. M. Ermolaev and G. I. Rashba, *Magnetoplasma Waves on the Surface of Semiconductor Nanotube with the Longitudinal Superlattice: International Conference "Physics of Disordered Systems"*, Lviv (2013) [in Russian].
31. A. M. Ermolaev and G. I. Rashba, *Phys. Solid State* **56**, 1696 (2014).
32. A. M. Ermolaev and G. I. Rashba, *Solid State Commun.* **192**, 79 (2014).
33. A. M. Ermolaev and G. I. Rashba, *Bulletin KhNU named after V. N. Karazin, Ser. "Physics"* **1135**, 10 (2014).
34. A. M. Ermolaev and G. I. Rashba, *Collective Excitations of Electron Gas on the Nanotube Surface in a Magnetic Field: Magnetoplasma and Spin Waves, Zero Sound, Ser. Handbook of Functional Nanomaterials,* Nova Science Publishers, New-York (2013), Vol. 4.
35. S. Iijima, *Nature* **354**, 56 (1991).
36. M. S. Dresselhaus, G. Dresselhaus, and P. C. Eklund, *Science of Fullerens and Carbon Nanotubes*, Acad. Press, New York (1996).
37. R. Saito, G. Dresselhaus, and M. S. Dresselhaus, *Physical Properties of Carbon Nanotubes,* Imperial College Press, London (1998).
38. L. I. Magarill, A. V. Chaplik, and M. V. Entin, *Usp. Fiz. Nauk* **175**, 995 (2005).
39. G. D. Mahan, *Phys. Rev. B* **69**, 125407 (2004).
40. A. Fetter, *Ann. Phys.* **88**, 1 (1974).
41. D. Sarma and J. J. Quinn, *Phys. Rev. B* **25**, 7603 (1982).
42. A. C. Tselis and J. J. Quinn, *Phys. Rev. B* **29**, 2021 (1984).
43. A. C. Tselis and J. J. Quinn, *Phys. Rev. B* **29**, 3318 (1984).
44. Q. Wei-ming and G. Kirczenow, *Phys. Rev. B* **36**, 6596 (1987).
45. K. Golden and G. Kalman, *Phys. Rev. B* **52**, 14719 (1995).
46. C. Yannouleas, E. Bogachek, and U. Landman, *Phys. Rev. B* **53**, 10225 (1996).
47. J. Lee, H. Kim, S. J. Kahng, and G. Kim, *Nature* **415**, 1005 (2002).
48. V. A. Geyler, V. A. Margulis, and A. B. Shorohov, *JETP* **115**, 1450 (1999).
49. T. Ando, *J. Phys. Soc. Jpn.* **74**, 777 (2005).
50. N. Tsuji, S. Takajo, and H. Aoki, *Phys. Rev. B* **75**, 153406 (2007).
51. Wu-Sheng Dai and M. Xie, *Phys. Rev. E* **70**, 016103 (2004).
52. V. L. Kuznetsov, I. N. Mazov, A. I. Delidovich, and E. D. Obraztsova, *Phys. Status Solidi B* **244**, 4165 (2007).
53. C. E. Cordeiro, A. Delfino, and T. Frederico, *Phys. Rev. B* **79**, 035417 (2009).
54. C. E. Cordeiro, A. Delfino, and T. Frederico, *Carbon* **47**, 690 (2009).
55. I. V. Krive, R. I. Shekhter, and M. Jonson, *Fiz. Nizk. Temp.* **32**, 1171 (2006) [*Low Temp. Phys*. **32**, 887 (2006)].
56. O. P. Volosknikova, D. V. Zavyalov, and S. V. Kryuchkov, *Magnetic Moment of a Quantum Cylinder with a Superlattice,* International Conference "*Radiation Physics of Solids*", Sevastopol, 645 (2007).
57. E. Bogachek and G. Gogadze, *JETP* **40**, 308 (1975).
58. A. M. Ermolaev, S. V. Kofanov, and G. I. Rashba, *Adv. Condens. Matter Phys.* **2011**, 901848 (2011).
59. V. Ya. Prinz, V. A. Seleznev, V. A. Samoylov, and A. K. Gutakovsky, *Microelectron. Eng.* **30**, 439 (1996).
60. V. Ya. Prinz, *Physica E* **24**, 54 (2004).
61. M. F. Lin and K. W. K. Shung, *Phys. Rev. B* **47**, 6617 (1993).
62. O. Sato, Y. Tanaka, M. Kobayashi, and A. Hasegawa, *Phys. Rev. B* **48**, 1947 (1993).
63. M. F. Lin and K. W. K. Shung, *Phys. Rev. B* **48**, 5567 (1993).
64. P. Longe and S. M. Bose, *Phys. Rev. B* **48**, 18239 (1993).
65. A. I. Vedernikov, A. O. Govorov, and A. V. Chaplik, *JETP* **120**, 979 (2001).
66. P. A. Eminov, Yu. V. Perepelkina, and Yu. I. Sezonov, *Phys. Solid State* **50**, 2220 (2008).
67. R. Z. Vitlina, L. I. Magarill, and A. V. Chaplik, *JETP* **133**, 906 (2008).
68. A. Morad and H. Khosravi, *Phys. Lett. A* **371**, 1 (2007).
69. L. D. Landau, *JETP* **32**, 59 (1957).
70. V. P. Silin, *JETP* **35**, 1243 (1958).
71. A.S. Kondrat'ev and A. E. Kuchma, *Electron Liquid of Normal Metals*, Leningrad State University, Leningrad (1980).
72. A. S. Kondrat'ev and A. E. Kuchma, *Lectures on the Theory of Quantum Liquids*, Leningrad State University, Leningrad (1989).
73. A. M. Ermolaev and N. V. Ulyanov, *Landau-Silin Spin Waves in Conductors with Impurity States,* Lambert, Saarbrucken (2012).
74. I. O. Kulik, *JETP Lett.* **11**, 275 (1970).
75. A. M. Ermolaev, G. I. Rashba, and M. A. Solyanik, *Vestnik KhNU, Ser. "Physics"* **914**, 24 (2010).
76. R. Z. Vitlina, L. I. Magarill, and A. V. Chaplik, *Pis'ma v JETP* **86**, 132 (2007) [in Russian].
77. P. A. Eminov, *JETP* **135**, 1029 (2009).
78. R. M. White, *Quantum Theory of Magnetism*, Springer-Verlag, Berlin-Heidelberg (2007).
79. E. Yanke, F. Emde, and F. Lyosh, *Special Functions,* Nauka, Moscow (1977).
80. A. Erdelyi, *Asymptotic Expansions, State Publishing House of Physical-Mathematical Literature*, Moscow (1962) [in Russian].
81. L. D. Landau and E. M. Lifshitz, *Statistical Physics,* Nauka, Moscow (1995), Part 1 [in Russian].
82. A. M. Ermolaev and G. I. Rashba, *Introduction to Statistical Physics and Thermodynamics*, KhNU named after V. N. Karazin, Kharkiv (2004) [in Russian].
83. F. M. Peeters and P. Vasilopoulos, *Phys. Rev. B* **46**, 4667 (1992).

84. A. P. Prudnikov, Yu. A. Brychkov, and O. I. Marichev, *Integrals and Series. Special Functions,* Nauka, Moscow (1983) [in Russian].
85. G. Bateman and A. Erdelyi, *Higher Transcendental Functions,* Nauka, Moscow (1974), Vol. 2 [in Russian].
86. A. M. Ermolaev, G. I. Rashba, and M. A. Solyanik, *Europ. Phys. J. B* **73**, 383 (2010).
87. P. M. Platzman and P. A. Wolff, *Waves and Interactions in Solid State Plasmas,* Academic Press, New York (1973).
88. D. Pines and P. Nozieres, *The Theory of Quantum Fluids,* W. A. Benjamin Inc., New York (1966).
89. A. M. Ermolaev, G. I. Rashba, and M. A. Solyanik, *Fiz. Nizk. Temp.* **37**, 1156 (2011) [*Low Temp. Phys.* **37**, 919 (2011)].
90. A. M. Ermolaev, G. I. Rashba, and M. A. Solyanik, *Physica B* **406**, 2077 (2011).
91. A. M. Ermolaev, G. I. Rashba, and M. A. Solyanik, *Fiz. Tverd. Tela* **53**, 1594 (2011) [in Russian].

Надгратка на поверхні нанотрубки

A. M. Ermolaev, G. I. Rashba

Наведено результати теоретичних досліджень термодинамічних, кінетичних та високочастотних властивостей електронного газу на поверхні нанотрубки у магнітному полі при наявності повздовжньої надгратки. Нанорозміри області руху електронів призводять до квантування енергії, а її неоднозв'язність у присутності магнітного поля — до ефектів, які є похідними від ефекту Ааронова–Бома. Показано, що кривина нанотрубки навіть у відсутності магнітного поля обумовлює нові макроскопічні осциляційні ефекти типу осциляцій де Гааза–ван Альфена, які пов'язані з квантуванням енергії поперечного руху електронів та з кореневими особливостями густини електронних станів на поверхні нанотрубки. У газовому наближенні розраховано термодинамічні потенціали та теплоємність електронного газу на трубці. Отримано формулу Кубо для тензора провідності електронного газу на поверхні нанотрубки. Визначено області згасання Ландау електромагнітних хвиль на трубці та теоретично передбачено биття на графіку залежності провідності від параметрів трубки. У гідродинамічному наближенні розглянуто плазмові хвилі на поверхні напівпровідникової нанотрубки з надграткою. Показано, що уздовж трубки з одним сортом носіїв можуть розповсюджуватися оптичні та акустичні плазмони. Досліджено електронні спінові хвилі на поверхні напівпровідникової нанотрубки з надграткою у магнітному полі. Розраховано спектри та області без зіткнення згасання цих хвиль. Показано, що в цих областях у випадку трубок малого радіуса з виродженим електронним газом згасання спінових хвиль відсутнє.

Ключові слова: нанотрубки, надгратка, магнітне поле, термодинамічні функції, динамічна провідність, плазмові хвилі, електронні спінові хвилі.